National Technical University of Athens

NATIONAL TECHNICAL UNIVERSITY OF ATHENS

SCHOOL OF NAVAL ARCHITECTURE AND MARINE ENGINEERING

DIPLOMA THESIS

POSITIONS OF BALANCE FOR RECTANGULAR SOLID BODIES OF INFINITE LENGTH CONTAINING LIQUID

MANIFAVA KONSTANTINA

SUPERVISOR: KONSTANTINOS J. SPYROU

ATHENS, SEPTEMBER 2017

Acknowledgments

I would like to thank my professor Konstantinos J. Spyrou for his advices, instructions and guidance he offered me during the planning and execution of the present thesis. His advices, which I value greatly, will help me throughout my professional carrier. He was always patient and supportive, with respect and trust towards my ideas and my work.

Furthermore, I would like to express my sincere gratitude to Panagiotis Anastopoulos for his help in conducting the experiment. He was willing to devote much time in order for our experiment to be successful, even though it was during the summer months. Ioannis Kontolefas devoted many hours in order to explain to me some details in the function of MatCont program. Professor Papalabrou offered me also valuable advices when I was confronted a problem with the MatLab code. I am grateful to them as well.

Finally, I would like to thank my loved ones, who have supported me throughout my university years. They have always been helpful, encouraging and tolerant. Their support was valuable to me.

Table of contents

Acknowledgements……2
Table of contents……3
List of figures……5
1.0 Introduction……7
2.0 Literature review……9
3.0 General Hydrostatics……11
3.1 General meanings……11
3.2 Static stability in small angles of heel……13
3.2.1 Angle of Loll……13
3.3 Large angles of heel……15
3.3.1 Righting arm and righting moment……15
4.0 Geometric calculations……17
4.1 Calculation of submerged volume……18
4.2 Study of diverse geometric positions of balance……19
4.3 Comparison of diagrams for a compact solid body……28
4.4 Results for a compact solid body……31
5.0 Energy approach……32
5.1 Historical information……32
5.2Expressions of potential energy……35
6.0 Theoretical background in non linear dynamics……43
6.1 Fixed points and stability……43
6.2 Bifurcations……44
6.2.1 Introduction……44
6.2.2 Pitchfork bifurcation……44
6.2.3 Saddle-node bifurcation……46
6.2.4Imperfect bifurcations……47
7.0 Results of the energy method……48

7.1 Diagrams presentation……48

7.2Conclusions……60

8.0 Experimental approach of stability……61

8.1 Experimental arrangement……61

8.2 Experimental procedure……62

8.3 Experimental results……62

8.4 Comparison of the results……65

9.0 Conclusions……68

References……70

List of figures

Figure 1: Static stability curve/GZ curve of a surface ship……12

Figure 2 (a): Negative stability- Angle < Angle of Loll……13

Figure 2 (b): Equilibrium at angle of Loll……13

Figure 2 (c): Positive stability- Angle> Angle of Loll……14

Figure 3: GZ curve for a ship having an angle of roll ……14

Figure 4: Typical cross curves of stability……16

Figure 5: Orthogonal prism at a=0……18

Figure 6i: 2 submerged angles (A, B)……19

Figure 6ii: One submerged angle (A)……20

Figure 6iii: 2 submerged angles (A, D)……21

Figure 7i: 2 submerged angles (A, B) for u<0.2h……22

Figure 7ii: One submerged angle (A) for u<0.2h……23

Figure 7iii: 2 submerged angles (A, D) for u<0.2h……24

Figure 8i: 2 submerged angles (A, B) for u>0.8h……25

Figure 8ii: One submerged angle (A) for u>0.8h……26

Figure 8iii: 2 submerged angles (A, D) for u>0.8h……27

Figure 9: GZ curve for r=0.1 by MatLab……29

Figure 10: GZ curve for r=0.1 by Mathematica……29

Figure 11: GZ curve for r=0.5 by MatLab……30

Figure 12: GZ curve for r=0.5 by Mathematica……31

Figure 13: Calculation of dynamic energy……33

Figure 14: Transverse surface of a cube having two submerged angles……34

Figure 15: Phase portrait……43

Figure 16: Supercritical Pitchfork Bifurcation for varied values of r……45

Figure 17: Supercritical Pitchfork bifurcation diagram……45

Figure 18: Subcritical Pitchfork bifurcation diagram……46

Figure 19: Saddle-node bifurcation as r is varied……..47

Figure 20: (α) Imperfect Bifurcation diagram. (b)Phase diagram for μ=5……..47

Figure 21: Diagram a-u for a square prism……48

Figure 22: Diagrams a-u for a square prism in different r……..51

Figure 23: Diagram a-r for a square prism and u=0.3……..51

Figure 24: Diagram a-u for a square prism and varied weight of void prism……..53

Figure 25: Diagram a-u for orthogonal prism with varying λ……55

Figure 26: Diagram a-u for an orthogonal prism……..55

Figure 27: Diagrams a-u for an orthogonal prism for varied r……57

Figure 28: Diagrams a-u for an orthogonal prism for varied W……..59

Figure 29: Mass density of the prisms……63

Figure 30:Values of the Fig. 31……63

Figure 31: Experimental measurements for the square prism……64

Figure 32: Experimental measurements for the orthogonal prism……64

Figure 33: Pictures of the prism in a vertical and a leaning position of balance……65

Figure 33: Longwise aspect of the prism in a leaning position of balance……65

Figure 35: Experimental results and mathematical results for the square prism in one graphic……..65

Figure 36: Experimental results and mathematical results for the orthogonal prism in one graphic…67

1. Introduction

The main subject of the present diploma thesis is the study of balance positions and stability in water, of prismatic objects containing liquid. The starting idea was based on the diploma thesis of Sakellariou (2013) who had dealt with a similar problem, however for homogeneous solid bodies [1]. We expanded this work by considering hollow prisms with internal liquid which makes the problem richer. Although one would tend to consider the problem as very simplistic and already solved, the fact is that the existing bibliography is not very extensive.

In the current study, floatability and stability are examined in depth for a prism with orthogonal sections of dimensions b*h. Both dimensions, as well as the ratio of specific gravity of the contained liquid versus the external fluid's constitute basic parameters of the problem and they appear in the final equations. Our results do not concern a particular case but can easily be implemented to an arbitrary orthogonal body since system's equations of rest and stability are parameterized with respect to prism's dimensions and specific gravity ratio.

The key method applied in our work is the so called "energy method". The energy method approaches the balance positions of a solid body and the stability of these positions, using its potential energy. In particular, we can determine the balance positions by finding the local 'maxima' and 'minima' of the potential function. Then, we check the stability by examining whether the energy tends to increase or decrease for small alternations of these positions. This approach constitutes a very interesting and reliable way to study the stability of a solid body.

In the early stages of our study, a question that emerged was the selection of the programming language to be used for the computations. Although Sakellariou had used Mathematica, we finally ended up using Matlab. Matlab has many add-ons, such as the versatile code named MatCont (embedded on MatLab), that allow someone to automate the analysis of data and summarize the results. We considered using Matcont for the automatic identification of the prism's equilibrium positions and their stability properties. At a later stage this was abandoned, but the use of MatLab was continued. Initially, we tried to recreate the analytical results of Sakellariou by writing a new MatLab code. After validating that our code was correct as our results were similar to Sakellariou's, we evolved our study and focused on prisms with internal liquid.

To validate our results referring to prisms with internal liquid we carried out experiments. In the experimental procedure, we used square and orthogonal prisms of specific geometry and infinite length. We assumed that prism's length is much larger than the other two dimensions so the finite length should not affect the experiment. These experiments confirmed the accuracy of our approach since they showed good coincidence with computational results.

A naval architect understands very well that the topic of this study constitutes an initial and basic form of the "damage stability" issue. The study of damage stability of a ship comes in use when the ship's watertight hull is affected in a way that allows water to flood any compartment within the ship's hull. Since this changes the stability parameters of the ship, the extent of which depends on the extent of damage and flooding, it is studied separately from intact stability [2]. Damage stability is of paramount importance for ship safety, therefore studies which improve our basic knowledge should be welcomed.

This diploma thesis consists of 10 chapters:

In particular, in chapter 2 the literature review is presented, summarizing briefly the scientific progress of the static ship stability theory throughout the centuries.

In chapter 3, we introduce some key concepts of hydrostatics. We analyze the way hydrostatic forces applied on a body combined with gravitational forces can affect the way they generate hydrostatic balance. Moreover, we are going to mention the theoretical background of static stability, referring to both the theory of small and large disturbances from equilibrium.

In chapter 4, we present a procedure of geometric determination of the positions of stability. The equations that are presented in this chapter are based on pure geometrical assumptions.

In chapter 5, we deal with the balance positions and their stability, using the energy formulation.

In chapter 6, we present some basic notions from nonlinear dynamics which play a key role in this study. In particular, we review the so called pitchfork bifurcation, both in its “perfect” and “imperfect” form.

In chapter 7, we present the results of the energy method. In particular, we have created several stability diagrams using Matlab code. Then, we interpret the obtained diagrams that in essence show the existence of bifurcation phenomena described in chapter 6.

In chapter 8, our experimental procedure and tools are described and our experimental results are analyzed.

In chapter 9, conclusions are drawn on the analytical and experimental results of the present diploma thesis.

Finally, bibliography and other relevant sources are cited.

2. Literature review

Archimedes was the first one who studied the stability positions of a parabolic segment of a body of revolution in water. The evolution of this theory was slow for many centuries until the 18th century, when Euler and Bouguer made many important discoveries on the subject. Dupin, Moseley and Froude expanded the study of stability even more in the 19th century.

Archimedes's study consists of the determination of possible «rest» positions of axis-symmetrical parabolic bodies on the water surface, both when their base is out of the water and when it is totally or partly submerged. The complete study of Archimedes can be found, e.g. in the book of Heath (2012) in English and also, in the so called "Archimedes palimpsest" (10th century) in Greek [3].

Two contemporary scientists Pierre Bouguer (1698-1758) and Leonhard Euler (1707-1783) are credited with the conception of a new, completely modernized approach, based for the first time on calculus, regarding ship hydrostatics and stability. They worked on these problems independently and without knowing of the other's work before their own large treatises were completed and were ready to be published. Bouguer's famous 'Traite du Navire' [4] appeared in 1746 soon after his return to France, while Euler's fundamental 'Scienta Navalis' [5] was published in 1749 after a major delay. Bougeur began his introduction of hydrostatics with the following explanation of the buoyancy force:

"The principle of hydrostatics, which must serve as a rule in this whole matter and which one must always have in mind, is that a body that floats on top of a liquid is pushed upward by a force equal to the weight of the water or liquid whose space it occupies".

This is tantamount to the Principle of Archimedes, only slightly rephrased. In the following chapter, the same result is also derived by integration of the hydrostatic pressure distribution over the submerged part of the hull surface. The pressure resultant or buoyancy force is then shown to be acting upward through the volume centroid of the submerged hull (or center of buoyancy), equal and opposite to the downward weight force (displacement) through the center of gravity of the hull.

For ship stability, for infinitesimally small angles of heel, Bouguer invented the metacenter as a stability criterion (the point of intersection of two infinitesimally adjacent buoyancy directions for a small angle of heel). For a stable ship, the center of gravity must not lie above the metacenter. Euler in the introduction to his «Scienta Navalis», begins his axiomatic foundation of hydrostatics with the statement:

"The pressure which the water exerts on a submerged body in specific points is normal to the body surface, and the force which any surface element sustains is equal to the weight of a vertical water column whose basis is equal to this element, whose height however equals the submergence of the element under the water surface."

All other results in ship hydrostatics can be derived from this axiom. For example, the buoyancy force in the Principle of Archimedes is deduced by pressure integration by means of calculus over the hull of an arbitrary body shape. Euler also applies Archimedean criteria to the hydrostatic stability of ships for infinitesimal angles of heel when he says:

“The stability, which a body floating in water in an equilibrium position maintains, is measured by the moment of the restoring force if the body is inclined from its equilibrium position by a given infinitely small angle.” [5]

An important contribution to the problems of floatation and in particular to the question of stability was made by Gilbert [7]. He used mainly the concept of metacenter, together with spherical harmonic developments, special functions defined on the surface of a sphere employed in solving partial differential equations, and Laplace transforms. Gilbert solved the problems of the floatation of an ellipsoid of arbitrary density and of a circular cylinder of arbitrary length-to-diameter ratio.

Amongst the contemporary investigators of the stability of prisms we distinguish Erdos, Schibler & Herdon [8] who studied stability of symmetric prisms (with square or triangular shape), by applying the energy approach,. They created diagrams for the angle of heel as a function of the ratio of the specific gravities of the solid and the liquid. After that, they expanded their study to the finding of stability positions for three-dimensional, symmetric, solid bodies by using the notion of buoyancy area.

Finally, it is spectacular that the problem of positions of rest and stability of prisms in water has remained relevant till our days as a research topic.

3.0 General hydrostatics

As we already know, when a body is being submerged in water, an amount of hydrostatic forces act on it. In this chapter, we analyze these forces in order to calculate their mathematical expressions. We also analyze the way the hydrostatic forces interact with the rest of the forces over the body and the way they achieve the final hydrostatic balance. Finally, we mention the theoretical background of the static balance, concerning both the theory of "small changes" and "big angles of heel".

3.1. Archimedes's principle

According to Archimedes' principle known as the Law of Floatation, when a body is floating freely in a fluid, the weight of the body equals the buoyancy, which is the weight of the fluid displaced. [9]

The buoyancy of a body immersed in a fluid is the vertical up thrust it experiences due to displacement of the fluid. The buoyancy is the resultant of all of the forces due to hydrostatic pressure on elements of the underwater portion. Now the hydrostatic pressure at a point in a fluid is equal to the depth of the point times the weight density of the fluid. For instance, the weight of a column of the fluid having unit cross section, length equal to the depth of immersion T, and weight density of the fluid w, is:

$$p = w \times T$$

We should now examine the pressure distribution around a rectangular block with volume $a \times b \times c$ floating squarely in a fluid with draught T. The pressures on the vertical faces of the block all cancel out and contribute nothing to the vertical resultant. The hydrostatic pressure at the bottom face is T×w and so the total vertical up thrust is this pressure multiplied by the area:

$$Up\ thrust = (T\ w) \times a \times b$$

But this is the displaced volume, $a \times b \times T$, times the weight density of the fluid, w, which is in accordance with the law of floatation.

The same is not quite true for the study of dynamic behavior of a vessel which depends upon mass rather than weight. However, it is force which causes changes and normally the single word displacement refers to a force and is defined by the symbol Δ. Thus:

$$\Delta = \rho \times g \times \nabla = w \times \nabla$$

The watertight volume of a ship above the waterline is called the reserve of buoyancy. It is clearly one measure of the ship's ability to withstand the effects of flooding following damage and is usually expressed as a percentage of the load displacement.

3.2 Static stability in small angles of heel

The easiest and handiest tool for analyzing a surface ship's stability is by graphs or curves. Since metacentric height is directly related to the righting lever (GZ) and angle of heel, the curve of static stability is a plot between the righting lever and angle of heel as we can see in Figure 1.

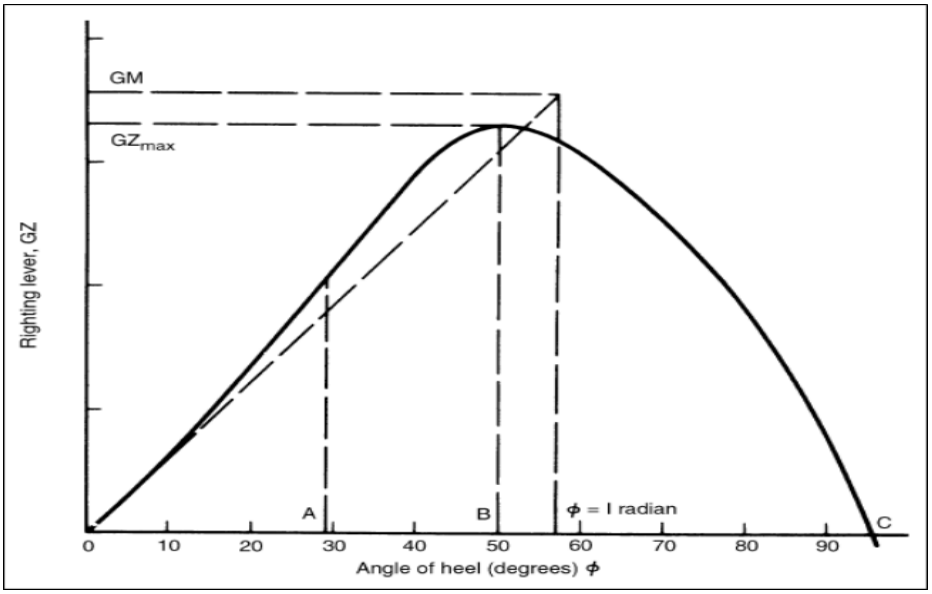

Figure 1: Static stability curve/GZ curve of a surface ship [10]

Some of the important information that can be derived from any GZ curve of a ship is mentioned below:

- If the curve intersects the origin, it means that there is no righting lever when the ship is upright. In other words, the ship has inherent positive initial stability.
- The maximum righting lever (GZ_{MAX}), represented by point 'B' in the graph is proportional to the largest static heeling moment that is required to bring the ship back to its upright position. In other words, the maximum righting lever when multiplied with the displacement of the ship, gives us the value of the maximum heeling moment that the ship can sustain without capsizing.
- The point where the GZ curve meets the horizontal axis (shown as 'C' in the figure), is called the ***point of vanishing stability***, since righting lever becomes zero at this point. So, any heel beyond this angle would result in a condition of negative stability. The distance between the origin and point of vanishing stability is called the ***range of stability*** of a ship. In the above case, the range of stability is from 0 degrees to some angle above 90 degrees.
- As the angle of heel increases, there comes a point when the deck of the ship immerses. This angle is called the ***angle of deck immersion***, and the corresponding point on the curve is called ***point of inflection***. This results a change in concavity of the curve. This can clearly be noted at point 'A' in the above curve.

Point of inflection does not play an important role in operational purposes, but it helps designers to make preliminary predictions regarding what changes in stability would be brought about if the design of a hull-form is altered.

- The total area under the static stability curve gives the amount of energy that the ship can absorb from external heeling forces (winds, waves, weight shifts, etc.) till it capsizes. Thus, it should not be assumed that a ship is stable enough only if the value of the maximum GZ is high. A GZ curve with a very high maximum value might not have the sufficient area, and as a result, the ship will capsize easily because it wouldn't be able to absorb enough energy before capsizing.
- If a tangent is drawn to the GZ curve at the origin, and an ordinate is drawn at 57.3 degrees (1 Radian), then the point of intersection of the tangent and the ordinate would

give the value of the initial metacentric height of the ship, as shown in the above figure. [11]

3.2.1 Angle of Loll

It may so occur that the initial metacentric height of the ship becomes negative. As a result of this, the ship is not stable in its upright condition, leading to a heeling moment, as shown in part (a) of Figure 2 below.

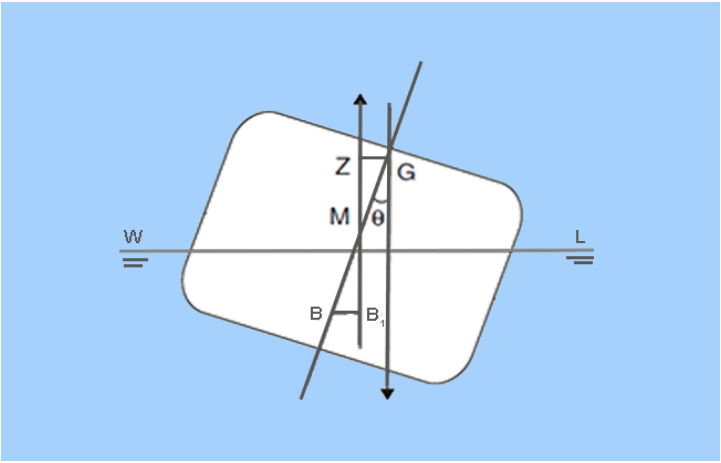

Figure 2 (a): Negative stability- Angle of heel< Angle of Loll [11]

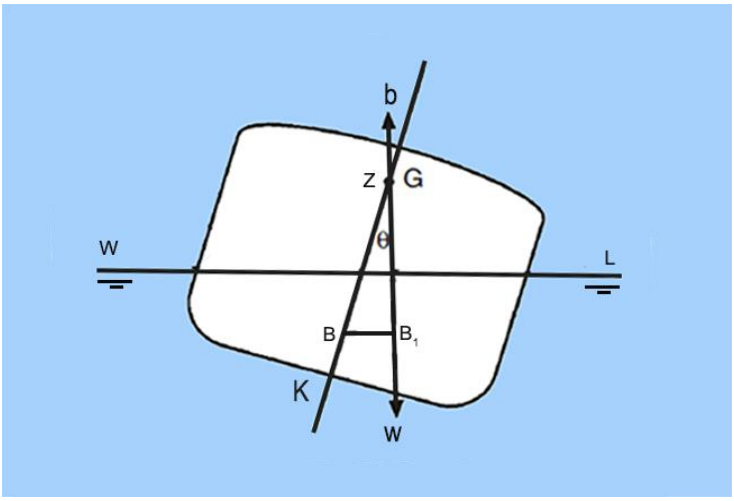

Figure 2 (b): Equilibrium at angle of Loll [11]

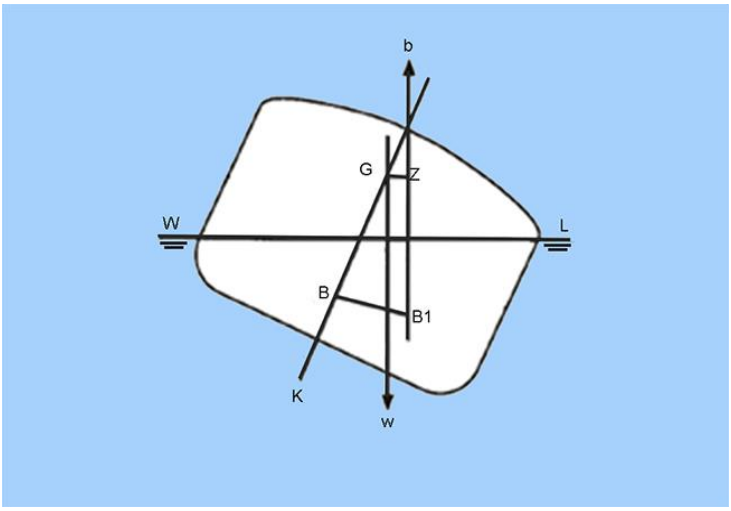

Figure 2 (c): Positive stability- Angle of heel> Angle of Loll [11]

As a result of the negative righting lever (GZ), the ship heels further upto an angle where the righting moment and righting lever, both, become zero. This angle at which this condition is achieved is called Angle of Loll, as shown in part (b) of Figure 2. The important thing to visualize here is that a condition of loll can be treated as a shift of the GZ curve from the origin (Figure 3).

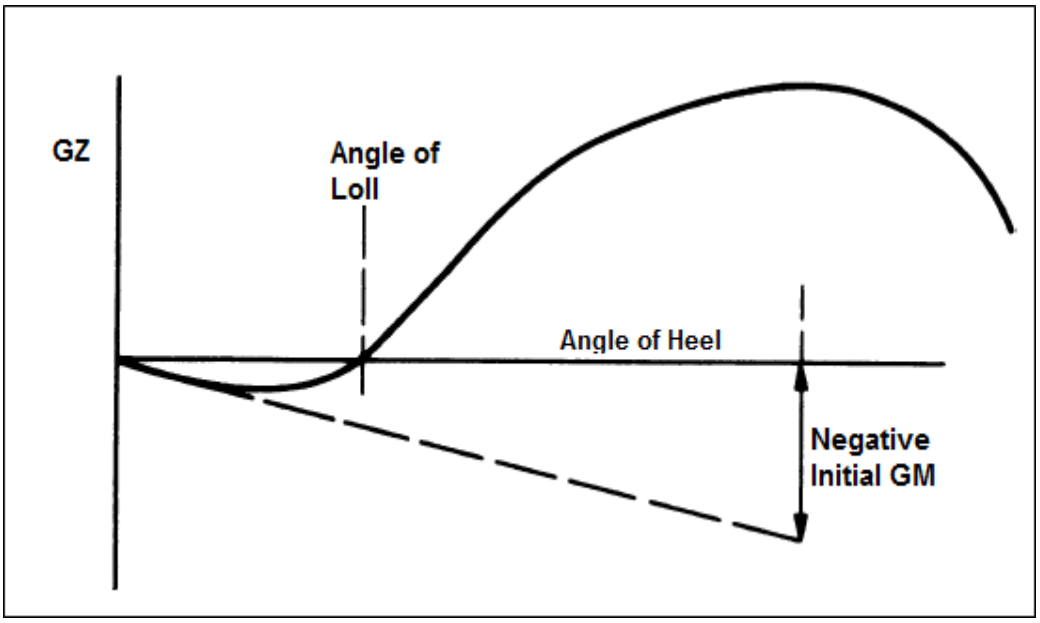

Figure 3: GZ curve for a ship having an angle of roll [11]

3.3 Large angles of heel

If upsetting forces that act upon ships in service, such as those caused by wind, waves, cargo handling, and turning, could not produce inclinations larger than a few degrees, the study of metacentric, or initial transverse statical stability would be sufficient for both ship designers and operators. However, ships can and do heel and roll to larger angles under the influence of large heeling moments. [12]

3.3.1 Righting arm and righting moment

Whatever the angle of heel, the proper measure of a ship's ability to return to upright is the righting moment, equal to the product of the ship's weight (Δ) and the righting arm (GZ). The difference between small and large angles of heel is due to the fact that at large angles the buoyant force vector does not pass through the metacentre (M). The reason is that, as the angle of heel increases beyond a few degrees, the path of the centre of buoyancy (B) departs from a circular arc of radius BM, becoming, for a hull with vertical walls around the waterline, parabolic. The consequence of this departure is that the righting arm is no longer related in any simple way to the metacentric height, that is, GZ is not equal to GM $\sin\varphi$, as it is in the case of very small angles of heel. In fact, no exact analytical formula is known that relates GM to the righting arms GZ for large angles, except for the very restrictive class of hull forms for which the centre of buoyancy traces a circular path when the vessel heels to any angle. The only practical hull forms satisfying these conditions are circular section pontoons and submarines whose hull forms are essentially bodies of revolution.

Once the righting arm, GZ, is determined for a given heel angle and loading condition the righting moment can be estimated as:

$$M_r = \Delta GZ = \Delta(BM - BG + MN)\sin\varphi$$

Where:

$BM\sin\varphi$: form stability

$BG\sin\varphi$: weight stability

$MN\sin\varphi$: residual stability

N is known as the pseudometacentre.

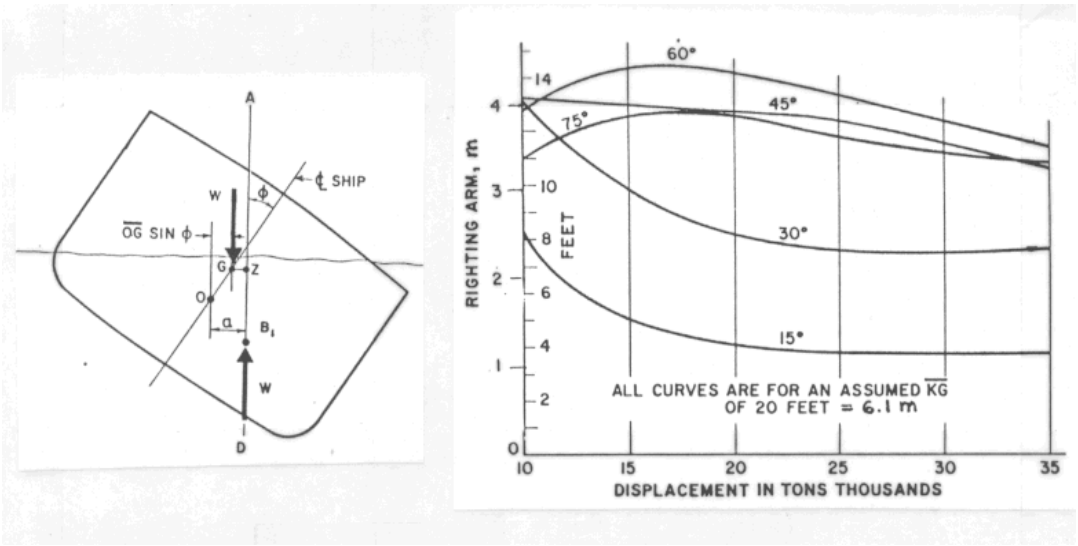

Figure 4: Typical cross curves of stability. [12]

4.0 Geometrical approach calculations

In this chapter, we are going to present the procedure for the geometric determination of possible positions of stability. The equations shown in this chapter are based purely on geometrical assumptions. However, in later chapters hydrostatics assumptions and reflections are introduced in order to create the final equations.

To start with, we need to mention our assumptions. According to Archimedes' principle, the weight of a body which balances on the surface of the water equals to the amount of the displaced water and the buoyancy force over the body. Considering the fact that the weight of the body is constant, If the immersed volume is not changed the buoyancy should also remain constant. Therefore, the submerged volume remains constant, no matter the heel of angle. Furthermore, we accept that the body is allowed to execute only roll motion. We exclude any transitional phenomenon between the positions of stability in order to simplify the problem. Finally, we make some extra assumptions concerning the internal liquid.

1. The free surface of the internal liquid is always parallel to the free surface of the external liquid – this of course results from the gravity of the liquid since we consider only static conditions, i.e. strictly speaking it is not an assumption.
2. The free surface of the internal liquid can be lower, equal or higher to the free surface of the external liquid.
3. We cannot consider a prism without weight because it is an unrealistic case. This would be an oversimplification and we could not compare against experimental results. So, we consider a prism that when being empty, it is going to have a draught equal to 30% of its height.

We consider a solid body in orthogonal shape, of infinite length, having the above characteristics. The parameters of the problem, with their symbols, are summarized below:

b: beam of the body

h: height of the body

l: length of the body ($l \to \infty$)

$\lambda = h/b$: ratio of the sides

T: draught of the body

a: angle of heel

u: height of the liquid inside the body

ρ_0: density of the body

ρ_1: density of the internal liquid

ρ_2: density of the external liquid

r: ratio of the density of the internal liquid to the density of the external liquid

g: gravity's acceleration

4.1 Calculation of submerged volume

Since we consider the submerged volume as constant, no matter the angle of heel, we start with the calculation of the submerged volume for zero angles. Since the length of the prism is infinite, the submerged area of every section remains constant. In Fig. 7 we see a random section of the prism:

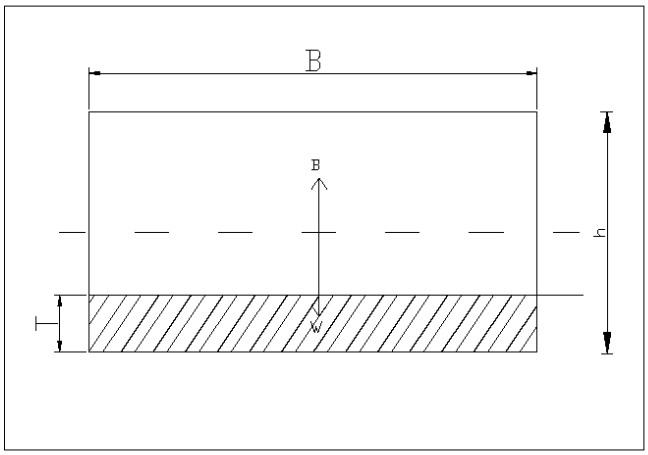

Figure 5: Orthogonal prism at a=0.

$$W = B\ (1)$$

$$W = m \times\ g\ = \rho \times\ V \times\ g = \rho_1 \times\ b\ \times \upsilon \times\ l\ \times g\ + W_{\text{prismatic}}$$

$$= \rho_1 \times\ b \times\ l \times\ \upsilon \times\ g\ +\ W_{\text{prismatic}} (2)$$

$$B =\ \rho\ \times V_{sub} \times\ g =\ \rho_0 \times\ (b\ T\ l) \times\ g\ (3)$$

We determine the weight of the body ($W_{\text{prismatic}}$)so that when the prism is empty, 30% of body's height will be submerged:

$$W_{prismatic} =\ \rho_0 \times\ (b\ 0.3h\ l)\ \times g\ (4)$$

$$(2), (4)\ \rightarrow\ W = \rho_1 \times\ b\ \times l\ \times \upsilon \times\ g\ +\ \rho_0 \times\ (b\ 0.3h\ l) \times\ g\ (5)$$

$$(1), (3), (5)\ \rightarrow\ T =\ r \times\ \upsilon\ +\ 0.3h$$

The submerged area of the orthogonal section is:

$$A =\ \ b\ \times (r \times\ \upsilon\ +\ 0.3h)$$

4.2 Study of diverse geometric positions of balance

To start with, we need to define geometrically the diverse positions of balance of the prism. We do this in order to find the mathematical equations giving the area, the centre of buoyancy and the coordinates of the four corners. So, the possible positions of heel are:

1. 2 submerged corners (A,B)
2. 1 submerged corner (A)
3. 2 submerged corners (A,D)
4. 3 submerged corners (A,C,D)

We have already calculated the submerged transverse area for zero angles as shown in chapter 4.1. We are going to calculate the area of the submerged part and assume that the two values are equal. As we already mentioned, this assumption is right because the value of the submerged area remains constant regardless of the heeling angle of the body. In this way, we find the first equation for each position. For the second equation, we use trigonometry. In particular, we use the definition of tangent angle. We have a different equation for any different angle of heeling. A 2 x 2 system of equations is written that helps us find the unknown variables. In our case, the unknowns are the distances y_1, y_2, x_1, x_2. These distances refer to the height of the internal liquid of the prism. If the height of the internal liquid overpasses the free surface, we consider as y_1 (or x_1) the height of the submerged part of the prism. If the distances are on the y-axis we use the variables y_1, y_2, otherwise we use the variables x_1, x_2(i.e see diagrams 8i, 8ii, 8iii, 9i, 9ii, 9iii, 10i, 10ii, 10iii). Finally, we use these variables to create the formulas of the volume and the centre of buoyancy of the submerged area.

- 2 submerged corners (A,B):

$$\frac{y_1+y_2}{2}b=b\,(ru + 0.3h)$$

$$tana = \frac{y_1 - y_2}{b}$$

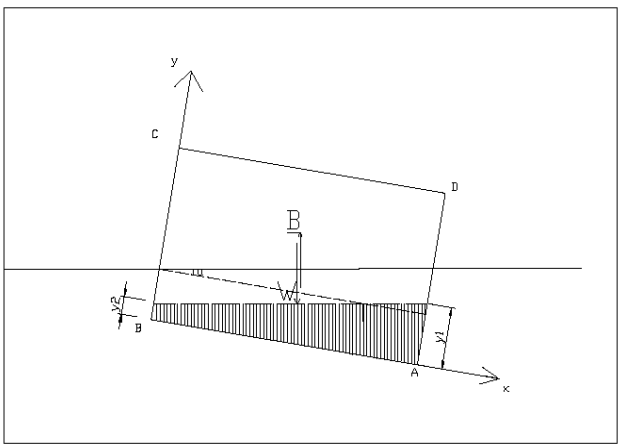

Figure 6i: 2 submerged corners (A, B)

So:

$$y_1 = (r \times \upsilon + 0.3h) + btana/2,$$
$$y_2 = (r \times \upsilon + 0.3h) - btana/2$$

$$Vc = (y_1 + y_2) \times \frac{b}{2}$$

$$Zc = \frac{3{y_2}^2 + 2{y_1}^2 + 6y_1y_2 - 2y_2}{3(y_1+y_2)} tan(a)$$

$$[(y_2 * b) * (y_1 + y_2/2) + b * (y_1 - y_2)/2 * 2y_1/3 = (y_1+y_2) * b/2 * zc\ ]$$

- 1 submerged corner (A):

$$x \times y/2 = b \times (r \times \upsilon + 0.3h)$$
$$tana = \frac{y}{x}$$

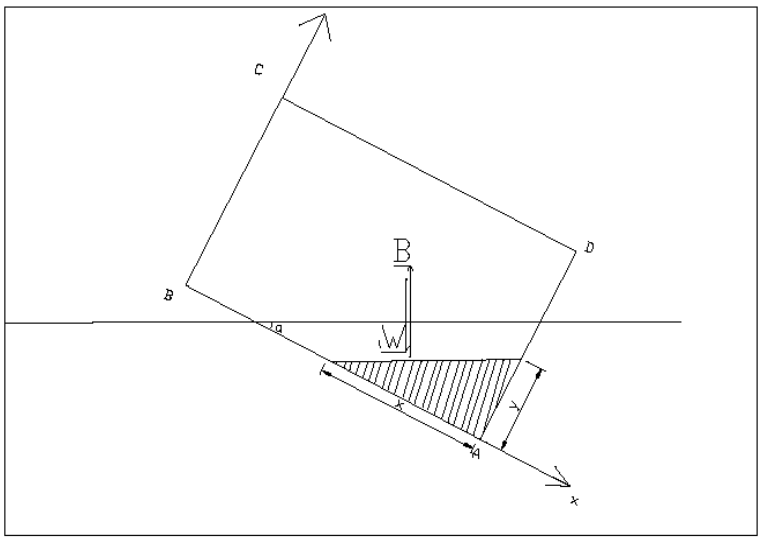

Figure 6ii: One submerged corner (A)

So:

$$x = \sqrt{\frac{2b(r\upsilon + 0.3h)}{tana}}$$
$$y = \sqrt{2b(r\upsilon + 0.3h)tana}$$

$$Vc = x \times y/2$$
$$Zc = 1/3 \times y$$

- 2submerged corners (A,D):

$$(x_1 + x_2)/2h = b \times (r \times v + 0.3h)$$

$$tana = \frac{x_1 - x_2}{h}$$

So:

$$x_1 = \frac{htana}{2} + \frac{b\,(r\,v + 0.3h)}{h},$$

$$x_2 = -\frac{htana}{2} + \frac{b\,(r\,v + 0.3h)}{h}$$

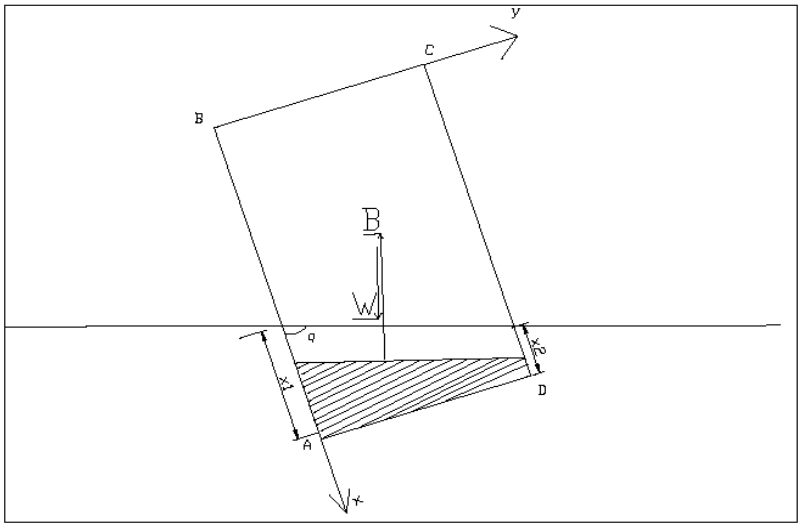

Figure 6iii: 2 submerged corners (A, D)

$$Vc = (x_1 + x_2)\,h/2,$$

$$Zc = \frac{2{x_1}^2 - {x_2}^2 + 2x_1x_2}{3(x_{1+}x_2)}cos(a)$$

- 3 submerged corners (A,C, D):

$$x_1 * h + \frac{(y_1 + h) * (b - x_1)}{2} = b\,(r\,v + 0.3h)$$

$$tan(a - \frac{pi}{2}) = \frac{b - x_1}{h - y_1} \rightarrow cot(a) = -\frac{b - x_1}{h - y_1}$$

$$(since\ \alpha = 90 + \varphi \rightarrow \varphi = \alpha - 90\ and\ tan(\varphi) = \frac{b - x_1}{h - y_1})$$

$$y_1 = h - \sqrt{\frac{2b(rh + ru - 0.7h)}{cota}},$$

$$x_1 = b + \sqrt{2bcota(rh + ru - 0.7h)}$$

$$Vc = x_1 * h + \frac{(y_1 + h) * (b - x_1)}{2}$$

$$Zc = \frac{y_1(b - x_1)^2 + \frac{2(b-x_1)(h-y_1)^2}{3} + x_1 h(2b - x_1)}{2x_1 h + (y_{1+} h)(b - x_1)}$$

Until now, we have studied the case of a body containing an intermediate amount of water. In this way, we neglect the extreme cases of a body containing very little or very much water (i.e. almost empty or almost full of water). We have made the assumption that the extreme cases concern a body containing water up to 20% of its height (υ<0.2h) or more than 80% of its height (υ>0.8h). The thick lines on the graphics constitute the free surfaces of the internal liquid. The mathematical expressions of the above cases are analyzed below:

<u>υ<0.2</u>

- 2 submerged corners (A,B):

$$x \times y/2 = b \times (r\upsilon + 0.3h)$$

$$tana = \frac{y}{x}$$

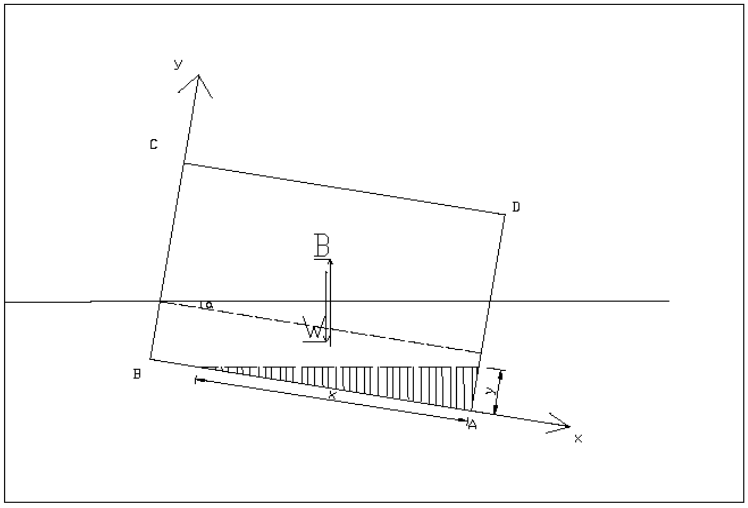

Figure 7i: 2 submerged corners (A, B) for u<0.2h

So:

$$x = \sqrt{\frac{2b(r\,v\ +\ 0.3h)}{tana}}$$

$$y = \sqrt{2b(r\,v\ +\ 0.3h)tana}$$

$$Vc = x \times y/2$$

$$Zc = 1/3 \times y$$

- 1 submerged corner (A):

$$x \times y/2\ =\ b\ \times (r\,v\ +\ 0.3h)$$

$$tana = y/x$$

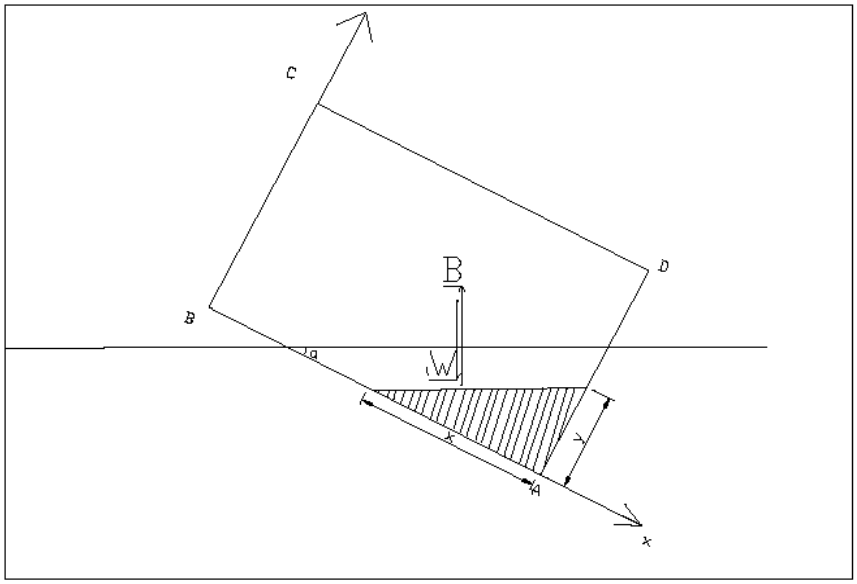

Figure 7ii: One submerged corner (A) for u<0.2h

So:

$$x = \sqrt{\frac{2b(r\,v\ +\ 0.3h)}{tana}}$$

$$y = \sqrt{2b(r\,v\ +\ 0.3h)tana}$$

$$Vc = x \times y/2$$

$$Zc = 1/3 \times y$$

- 2submerged corners (A,D):

$$x \times y/2\ =\ b \times\ (r\,v\ +\ 0.3h)$$

$$tana = x/y$$

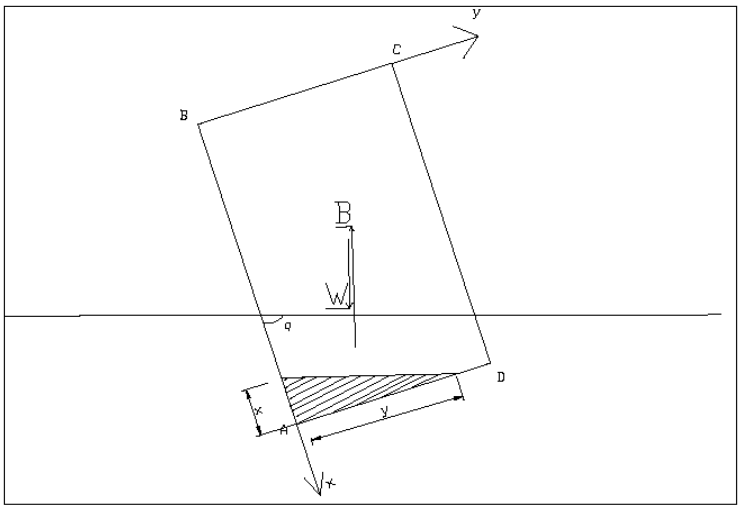

Figure 7iii: 2 submerged corners (A, D) for u<0.2h

So:

$$y = \sqrt{\frac{2b(r\,v\ +\ 0.3h)}{tana}}$$

$$x = \sqrt{2b(r\,v\ +\ 0.3h)tana}$$

$$Vc = X \times Y/2$$

$$Zc = 1/3 \times Y$$

- 3 submerged corners (A,C, D):

$$xy/2\ =\ b\,(r\,v\ +\ 0.3h)$$

$$tan(a - pi/2) = X/Y\ \rightarrow cot(a) = -X/Y$$

$$(since\ \alpha = 90 + \varphi\ \rightarrow\ \varphi = \alpha - 90\ and\ tan(\varphi) =\ (b - x\_1)/(h - y\_1\ )\ )$$

$$y1 = \sqrt{-\frac{2b(r\,v\ +\ 0.3h)}{cota}},$$

$$x1 = \sqrt{-2b(r\,v\ +\ 0.3h)cota}$$

$$Vc =\ X \times Y/2$$

$$Zc = 1/3 \times X$$

<u>υ>0.8</u>

- 2 submerged corners (A,B):

$$h \times b\ -\ (y_1 \times y_2)/2\ =\ b \times\ (r\,v\ +\ 0.3h)$$

$$tana = \frac{y}{x}$$

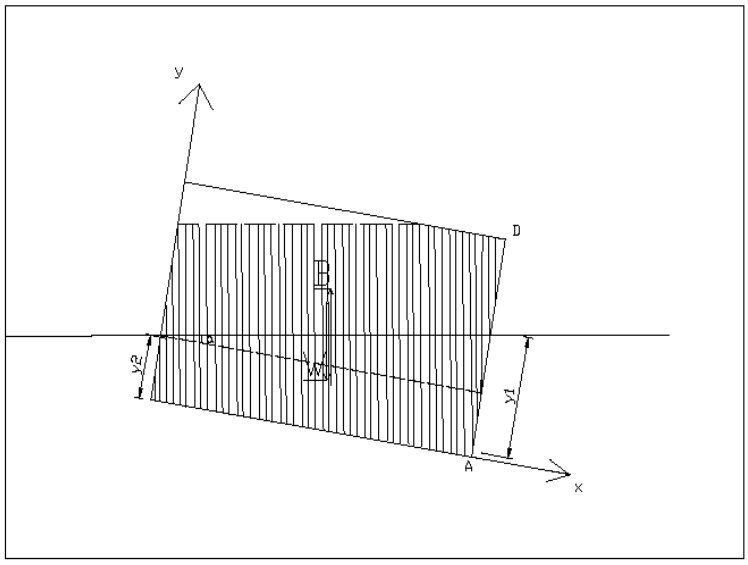

Figure 8i: 2 submerged corners (A, B) for u>0.8h

So:

$$y1 = \sqrt{\frac{2b(0.7h - rv)}{tana}}$$

$$y2 = \sqrt{2b(0.7h - rv)tana}$$

$$Vc = y_1 \times y_2/2$$

$$Zc = 1/3 \times y_2$$

- 1 submerged corner (A):

$$h \times b - \frac{x \times y}{2} = b \times (r\,v + 0.3h)$$

$$tana = \frac{y}{x}$$

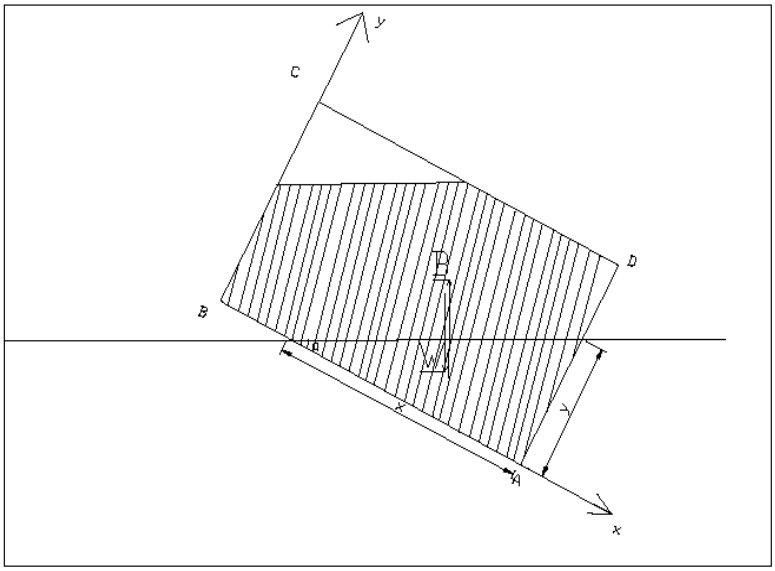

Figure 8ii: One submerged corner (A) for u>0.8h

So:

$$x = \sqrt{\frac{2b(0.7h - rv)}{tana}}$$

$$y = \sqrt{2b(0.7h - rv)tana}$$

$$Vc = x \times y/2$$

$$Zc = 1/3 \times y$$

- 2submerged corners (A,D):

$$h \times b - \frac{x \times y}{2} = b \times (r\,v + 0.3h)$$

$$tana = \frac{x}{y}$$

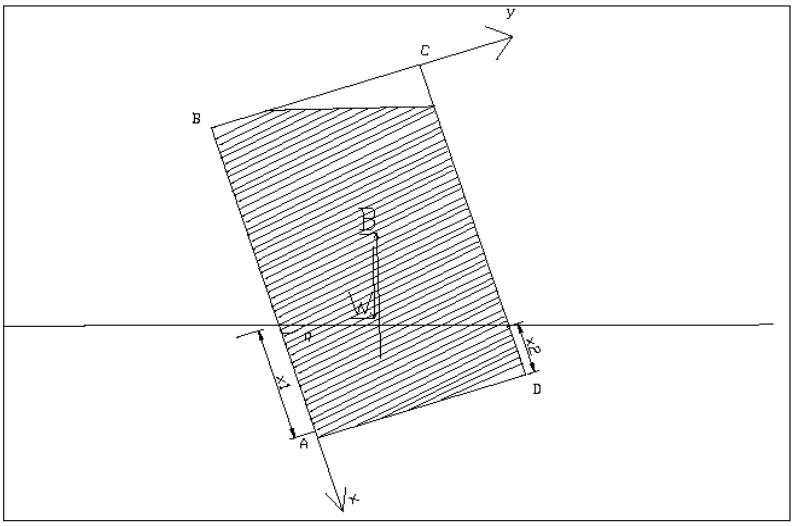

Figure 8iii: 2 submerged corners (A, D) for u>0.8h

So:

$$y = \sqrt{\frac{2b(0.7h - rv)}{tana}}$$

$$x = \sqrt{2b(0.7h - rv)tana}$$

$$Vc = X \times Y/2$$

$$Zc = 1/3 \times Y$$

- 3 submerged corners (A,C, D):

$$h \times b - \frac{x \times y}{2} = b \times (r\,v + 0.3h)$$

$$tan(a - \frac{pi}{2}) = \frac{X}{Y} \rightarrow cot(a) = -\frac{X}{Y}$$

$$(since\ \alpha = 90 + \varphi \rightarrow \varphi = \alpha - 90\ and\ tan(\varphi) = \frac{b - x_1}{h - y_1})$$

$$y_1 = \sqrt{-\frac{2b(0.7h - rv)}{cota}},$$

$$x_1 = \sqrt{-2b(0.7h - rv)cota}$$

$$Vc = X \times Y/2$$

$$Zc = 1/3 \times X$$

4.3Comparison of diagrams for a compact solid body

The diagrams that we are going to compare are righting arm (GZ) diagrams. We derive the GZ expressions for a solid body containing solid material and the corresponding diagrams. Here, we must also mention that the case of r<0.5 is different from the case of r>0.5. When the centre of buoyancy of the prism is under the free surface of the external fluid (r>0.5), the prism has different positions of balance and we should study different geometrical conditions. For instance, for r<0.5, the body can only have one or two submerged angles but for r>0.5 the positions change and the body can have two or three submerged angles. This is reasonable because in reality, when we study the problem of r>0.5, we study the symmetrical of r<0.5. In both cases, the prism can have two submerged angles but the domain of definition that the prism balances in this position changes.

The analysis until now is accurate for both a body containing solid and liquid but it is mainly focused on liquid context. For a more detailed description of the first case, we encourage you to read the thesis of A. Sakelariou [1].

1. If r<0.5:

A. Two submerged angles (A, B)

$$GZ = (sin(a))/(24\,h\,r)\,(2 - 12h^2r + 12h^2r^2 + tan^2(a))$$

$$0 \le a \le tan^{-1}(2hr)$$

B. One submerged angle (A)

$$GZ = (sin(a))/6(3h - 3cot(a) + 2\sqrt{2}cot(a)\sqrt{(hrcot(a))} - 2\sqrt{2}\,\sqrt{(hrtan(a))}$$

$$tan\text{^}(-1)\,(2hr) \le a \le tan - 1(h/(2r))$$

Γ. Two submerged angles (A,D)

$$GZ = (sin(a)cot(a))/24r(2(h^2 + 6(r-1)r) + h^2cot^2(a))$$

$$tan^{-1}\,(h/(2r)) \le a \le \pi/2$$

So, for r=0.1:

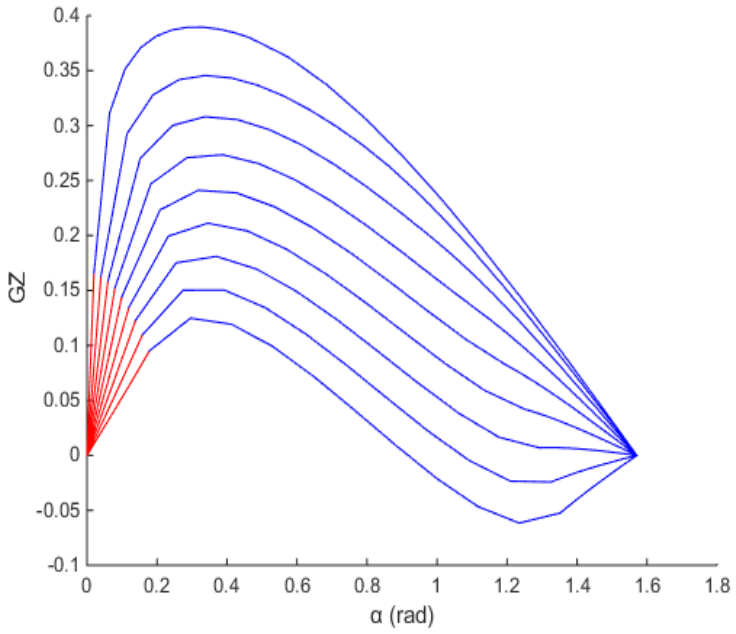

Figure 9: GZ curve for r=0.1 by MatLab

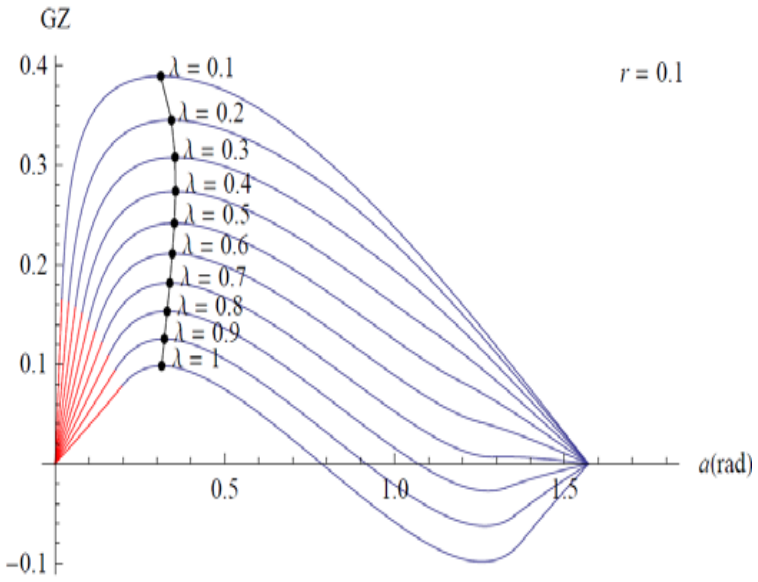

Figure 10: GZ curve for r=0.1 by Mathematica

2. If r>0.5:

A. Two submerged angles (A,B)

$$GZ = (sin(a))/(24\,h\,r)(2(1+6h^2r(r-1))+tan^2(a))$$

$$0 \le a \le tan^{-1}(2h(1-r))$$

B. Three submerged angles (A, B, D)

$$GZ = (sin(a))/(6rtan(a)\sqrt{(r(1-r))}\quad((1-r)\,(cot(a)(-2\sqrt{2}\,h\,(1-r) + 3\sqrt{(h(1-r)tan(a))}) - h(-2\sqrt{2}\,tan(a) + 3\sqrt{(h(1-r)tan(a))})$$

$$tan^{-1}\,(2h(1-r)) \le a \le tan^{-1}(h/(2(1-r)))$$

Γ. Two submerged angles (A, D)

$$GZ = (sin(a)cot(a))/24r(2(h^2+6(r-1)r)+h^2cot2(a))$$

$$tan^{-1}\,(h/(2(1-r))) \le a \le \pi/$$

So, for r=0.5:

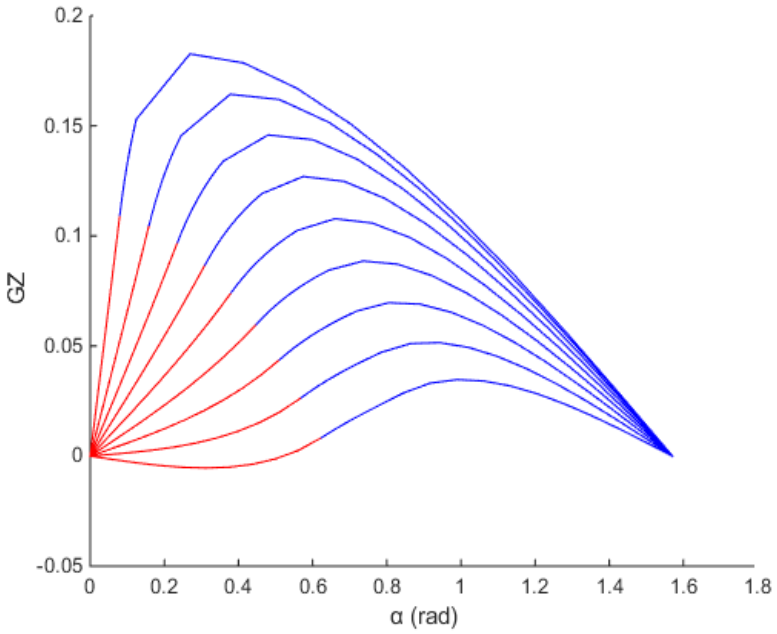

Figure 11: GZ curve for r=0.5 by MatLab

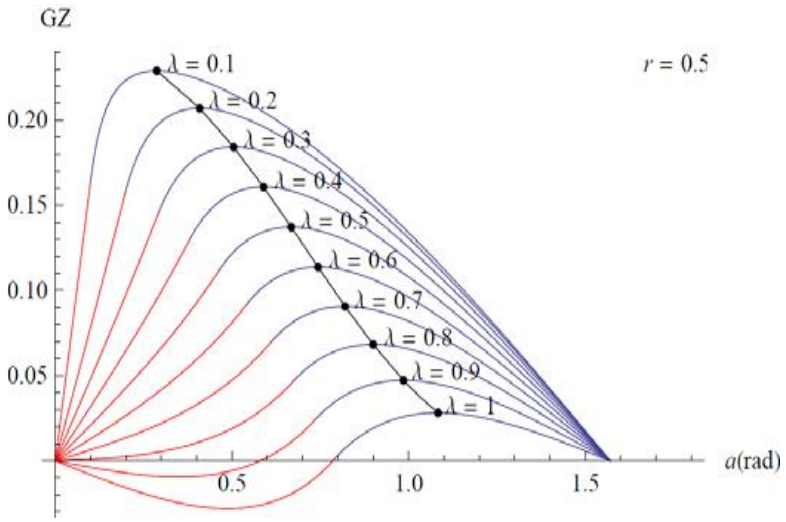

Figure 12: GZ curve for r=0.5 by Mathematica

4.4 Results and comments

Here, we are able to present the first results of the geometrical analysis:

- There is a clear symmetry between the case of u<0.2h and the case of u>0.8h.
- The geometrical symmetry is reasonable and expected because the one position is the reversed of the other.
- In the case of one submerged corner, the equations are similar no matter the height of the internal liquid.
- The symmetry between the three submerged corners and the one submerged corner applies everywhere no matter the height of the internal liquid.

Geometrical approach was proved to be a convenient and clear way to approach the equations. However, we should mention that the approach used in the present thesis is different from that of Sakelariou who had used an analytical method based on the affine transformation, for both rotation and translation, in order to find the final coordinates of the prism's corners. The analytical method is a grinding and more complicated way but has the ability to approach shapes with complex geometry. In our case, we are going to deal with an orthogonal shape so the geometry is easily known.

5.0 Energy approach

In this chapter, we approach a solid body's balance positions and their stability using its energy. We are going to use mathematical expressions for the geometry of the prism in order to find the energy functions and then calculate the balance positions. By creating some more equations, we will be able to understand which positions are finally stable and which are not. The final results are being presented in diagrams. The energy approach constitutes a very interesting and reliable way to study the stability of a solid body.

5.1 Theoretical background

The behavior of floating symmetrical objects is still a crucial issue for the international science community. Great scientists such as Gilbert (1991), Erdos et al. (1992), Megel&Kliava (2010) have published interesting papers about the issue no matter its classic character.

For instance, Erdos has published a report about a cube having ratio of densities between 0 and 0.5. For values till α=0.211, the cube balances in the horizontal position. However, by the value $\alpha=\frac{1}{6}$, there is already a second stable position where the diagonal of the cube is in the vertical position. This second position remains constant during the rest modifications of the ratio α. Despite this fact, the first, symmetrical position is more stable. By the value α=0.211, the symmetrical position becomes unstable and the cube balances in a heeling position. When having the value α=0.25, it happens a sudden changeover from the last position in a new one that the three edges of the cube are emerged and the last one is immersed. This position has started to coexist with the previous heeling position by the value a=0.2265 and disappears around the value α=0.2377. [2]

Huygens was the first researcher who approached the issue of ship stability. He started by expressing the summation of the potential energy of both the prism and the displaced water as a function of the angle of heel and the horizontal distance between the centre of mass and the free surface; as a consequence potential energy is a function of the ratio of densities. Consequently, we can determine the balance positions by finding the local minimum and maximum of the potential energy function. Furthermore, we can check the stability of balance positions that we have determined, by examining whether the energy tends to increase or decrease for small modifications.

In particular, let's define that whenever the centre of gravity is in the position of free surface, the potential energy is equal to zero. Then, the potential energy of the prism is determined by the rise of its centre of gravity:

$$U_1 = g \times \rho \times V \times z$$

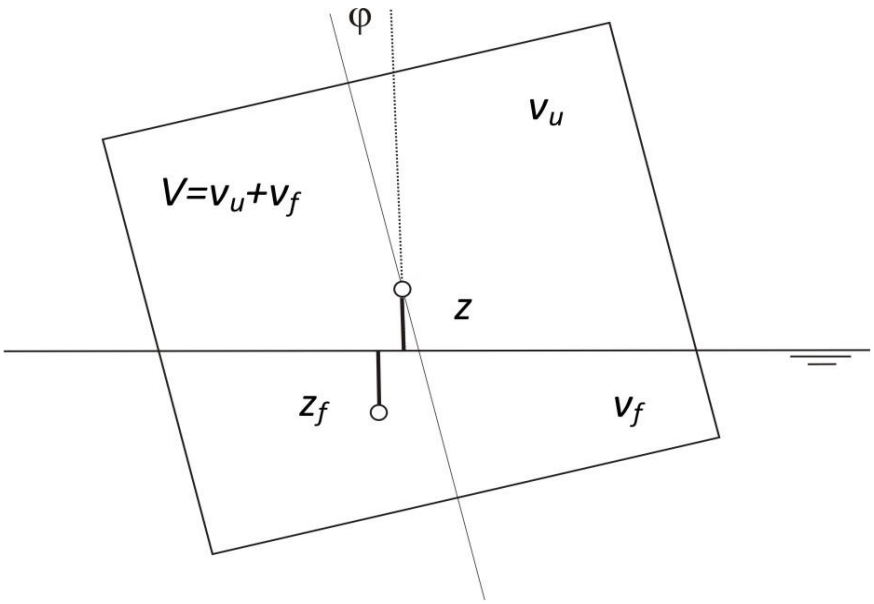

Figure 13: Calculation of potential energy

The potential energy of the displaced liquid, due to its rise on the free surface, is going to be:

$$U_2 = -g \times \rho_f \times v_f \times z_f$$

The total potential energy is calculated as the summation of the above values of potential energy (Fig. 13):

$$E = U_1 + U_2 = g \times \rho_f \times (\alpha V z - v_f z_f)$$

The balance positions arise by the two equations below that can calculate the local maximum and minimum:

$$\frac{\partial E(z,\varphi)}{\partial z} = 0, \frac{\partial E(z,\varphi)}{\partial \varphi} = 0$$

Amongst the possible balance positions for a particular value of the ratio of densities, the stable positions are those that their total energy tends to increase for small modifications of the parameters z, ϕ. We can mathematically express this condition in this way:

$$\delta E = \sum_{i=1}^{n} \sum_{j=1}^{n} \frac{\partial E}{\partial q_i} \frac{\partial E}{\partial q_j} \delta q_i \delta q_j > 0$$

The derivatives concern the balance position under examination. In our case, we have q_1=z, q_2=ϕ. So, it is n=2 and the problem is importantly simplified. In the general case, there is the demand that the hessian determinant ($\frac{\partial E}{\partial q_i}\frac{\partial E}{\partial q_j}$)has to present only positive eigenvalues, in order to satisfy the above equations.

Now, we have to make some calculations focusing on our case.

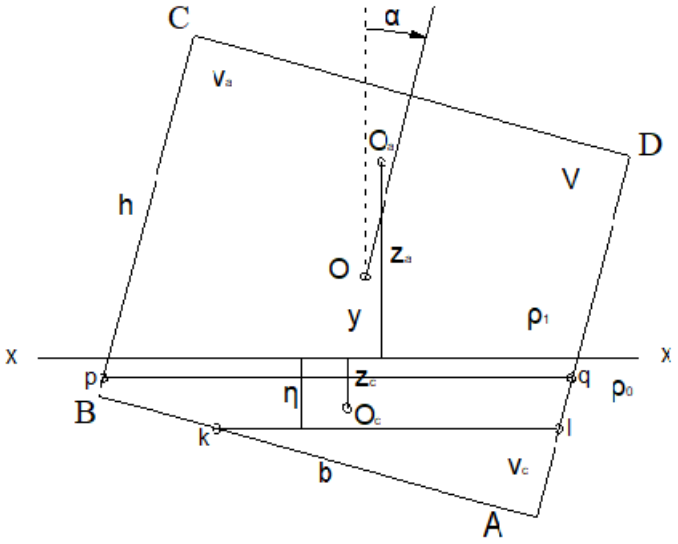

Figure 14: Transverse surface of a cube having two submerged angles [4]

In Fig. 14, we can see the transverse surface of a cube having the following characteristics:

x:the axis of the free surface of a liquid

O : the centre of gravity of the whole body

O_a : the centre of gravity of the emerged part of the body

O_c : the centre of gravity of the submerged part of the body

z_c:the ordinate of the centre of gravity of the submerged part of the body

y_{iw}:the ordinate of the centre of gravity of the internal water

y_s:the ordinate of the centre of gravity of the void body

ρ_s: density of the body

ρ_{iw}: density of the internal liquid

ρ_f: density of the external liquid

r: ratio of the density of the internal liquid to the density of the external liquid

V_c: the submerged volume of the body

V_{iw}: the volume of the internal water

V_S: the volume of the void body

For the following energy analysis, we consider the free surface of the external liquid as the level of zero dynamic energy of the system.

The potential energy of the solid body is:

$$U_S = g \times (\rho_{iw} V_{iw} y_{iw} + \rho_s V_s y_s)$$

The potential energy of the displaced liquid is:

$$U_l = -g \times \rho_f \times V_c \times z_c$$

After some more calculations, the potential energy of the solid body is:

$$U_s = g \times (\rho iw Viw\ yiw + \rho s\ Vs\ ys) = g \times (\rho iw Viw\ yiw + W/g\ ys)$$
$$= g \times \rho s \times Vs \times ys + W \times h/2$$

We find the total potential energy to be:

$$E = U_s + U_l = g \times \rho_f \times (r\ V_{iw} y_{iw} - V_c z_c) + W \times h/2$$

We can assume that:

$y_s = h/2$:centre of gravity of an orthogonal prism

$V_{iw} = b\ v$: volume of the internal water

$y_{iw} = v/2$:centre of area of the internal water

So, finally:

$$E = g \times \rho_f (r \times b \times u^2/2 - V_c \times z_c) + W \times h/2$$

The energy is usually expressed as a function of the angle of heel α and the centre of gravity of the whole body. Here, we have a different, more complicated problem so we are going to express it as a function of the angle α and the height of the internal liquid υ.

5.2 Expressions of the potential energy

In this chapter, we are going to express the equations of dynamic energy for the system solid body-internal liquid-external liquid in each case. We have considered a prism having dimensions b x h and we need to express its dynamic energy for each different position that it can balance. In order to achieve it, we have to use the geometrical expressions that we have exported in a previous chapter. The diverse cases are mentioned below:

1) Two submerged angles (A, B)
2) One submerged angle (A)
3) Two submerged angles (A, D)
4) Three submerged angles (A, B, D)

We remind that each above case has an energy expression for u< 0.2h, a second expression for 0.2h <u<0.8h and a last expression for u>0.8h.Because of the complexity and the quantity of these expressions, we are just going to mention some of them for

reasons of completeness. We will adduce the expressions of the main case for 0.2h< u<0.8h.

1) Two submerged angles (A, B)

$$E = (r * u\text{^}2)/2 + (3 * h\text{^}2)/20 - (tan(a) * ((3 * h)/10 + r * u) * (tan(a) - (3 * h)/5 + 3 * ((3 * h)/10 - tan(a)/2 + r * u)\text{^}2 + ((3 * h)/10 + tan(a)/2 + r * u)\text{^}2 - 2 * r * u + ((3 * h)/10 + tan(a)/2 + r * u) * ((9 * h)/5 - 3 * tan(a) + 6 * r * u)))/((9 * h)/5 + 6 * r * u)$$

By the derivatives of the dynamic energy we find the below equations. In this way, for a particular height of the internal liquid, we find the angle of balance.

∂E/∂a= Ea=- (7*(tan(a)/2 - 9/50)*(tan(a)^2/2 + 1/2))/6 - ((tan(a)/2 + 9/50)*(tan(a)^2/2 + 1/2))/2 =0

∂E/∂u=Eu = r*u - (r*tan(a)*(tan(a) - (3*h)/5 + 3*((3*h)/10 - tan(a)/2 + r*u)^2 + ((3*h)/10 + tan(a)/2 + r*u)^2 - 2*r*u + ((3*h)/10 + tan(a)/2 + r*u)*((9*h)/5 - 3*tan(a) + 6*r*u)))/((9*h)/5 + 6*r*u) - (tan(a)*((3*h)/10 + r*u)*(6*r*((3*h)/10 - tan(a)/2 + r*u) - 2*r + 8*r*((3*h)/10 + tan(a)/2 + r*u) + r*((9*h)/5 - 3*tan(a) + 6*r*u)))/((9*h)/5 + 6*r*u) + (6*r*tan(a)*((3*h)/10 + r*u)*(tan(a) - (3*h)/5 + 3*((3*h)/10 - tan(a)/2 + r*u)^2 + ((3*h)/10 + tan(a)/2 + r*u)^2 - 2*r*u + ((3*h)/10 + tan(a)/2 + r*u)*((9*h)/5 - 3*tan(a) + 6*r*u)))/((9*h)/5 + 6*r*u)^ =0

2) *One submerged angle (A)*

$$E = (r * u\text{^}2)/2 + (3 * h\text{^}2)/20 - (tan(a) * (((3 * h)/5 + 2 * r * u)/tan(a))\text{^}(1/2) * ((3 * h)/5 + 2 * r * u))/6$$

$$Ea = (((3 * h)/5 + 2 * r * u)\text{^}2 * (tan(a)\text{^}2 + 1))/(12 * tan(a) * (((3 * h)/5 + 2 * r * u)/tan(a))\text{^}(1/2)) - ((((3 * h)/5 + 2 * r * u)/tan(a))\text{^}(1/2) * ((3 * h)/5 + 2 * r * u) * (tan(a)\text{^}2 + 1))/6$$

$$Eu = r * u - (r * tan(a) * (((3 * h)/5 + 2 * r * u)/tan(a))\text{^}(1/2))/3 - (r * ((3 * h)/5 + 2 * r * u))/(6 * (((3 * h)/5 + 2 * r * u)/tan(a))\text{^}(1/2))$$

3) *Two submerged angles* (A, D)

$$E = (r * u\text{^}2)/2 + (3 * h\text{^}2)/20 - (h * cos(a) * ((((3 * h)/10 + r * u)/h + (h * tan(a))/2) * ((2 * ((3 * h)/10 + r * u))/h - h * tan(a)) - (((3 * h)/10 + r * u)/h - (h * tan(a))/2)\text{^}2 + 2 * (((3 * h)/10 + r * u)/h + (h * tan(a))/2)\text{^}2))/6$$

$$Ea = (h * sin(a) * ((((3 * h)/10 + r * u)/h + (h * tan(a))/2) * ((2 * ((3 * h)/10 + r * u))/h - h * tan(a)) - (((3 * h)/10 + r * u)/h - (h * tan(a))/2)\text{^}2 + 2 * (((3 * h)/10 + r * u)/h + (h * tan(a))/2)\text{^}2))/6 - (h * cos(a) * (h * (((3 * h)/10 + r * u)/h - (h * tan(a))/2) * (tan(a)\text{^}2 + 1) + h * (((3 * h)/10 + r * u)/h + (h * tan(a))/2) * (tan(a)\text{^}2 + 1) + (h * ((2 * ((3 * h)/10 + r * u))/h - h * tan(a)) * (tan(a)\text{^}2 + 1))/2))/6$$

$$Eu = r * u - (h * cos(a) * ((6 * r * (((3 * h)/10 + r * u)/h + (h * tan(a))/2))/h - (2 * r * (((3 * h)/10 + r * u)/h - (h * tan(a))/2))/h + (r * ((2 * ((3 * h)/10 + r * u))/h - h * tan(a)))/h))/6$$

4) *Three submerged angles* (A, B, D)

$$E = (r*u\text{^}2)/2 + (3*h\text{^}2)/20 - ((h*(2\text{^}(1/2)*(cot(a)*(h*r - (7*h)/10 + r*u))\text{^}(1/2) - 1) - (2\text{^}(1/2)*(2*h - ((2*h*r - (7*h)/5 + 2*r*u)/cot(a))\text{^}(1/2))*(cot(a)*(h*r - (7*h)/10 + r*u))\text{^}(1/2))/2)*(2*cot(a)*(h - ((2*h*r - (7*h)/5 + 2*r*u)/cot(a))\text{^}(1/2))*(h*r - (7*h)/10 + r*u) - h*(2\text{^}(1/2)*(cot(a)*(h*r - (7*h)/10 + r*u))\text{^}(1/2) - 1)*(2\text{^}(1/2)*(cot(a)*(h*r - (7*h)/10 + r*u))\text{^}(1/2) + 1) + (2*2\text{^}(1/2)*(cot(a)*(h*r - (7*h)/10 + r*u))\text{^}(1/2)*(2*h*r - (7*h)/5 + 2*r*u))/(3*cot(a))))/(h*(2*2\text{^}(1/2)*(cot(a)*(h*r - (7*h)/10 + r*u))\text{^}(1/2) - 2) - 2\text{^}(1/2)*(2*h - ((2*h*r - (7*h)/5 + 2*r*u)/cot(a))\text{^}(1/2))*(cot(a)*(h*r - (7*h)/10 + r*u))\text{^}(1/2))$$

$$
\begin{aligned}
Ea = {} & ((h*(2\text{^}(1/2)*(cot(a)*(h*r-(7*h)/10+r*u))\text{^}(1/2)-1) \\
& -(2\text{^}(1/2)*(2*h-((2*h*r-(7*h)/5+2*r \\
& *u)/cot(a))\text{^}(1/2))*(cot(a)*(h*r-(7*h)/10+r \\
& *u))\text{^}(1/2))/2)*(2*(cot(a)\text{^}2+1)*(h-((2*h*r-(7 \\
& *h)/5+2*r*u)/cot(a))\text{^}(1/2))*(h*r-(7*h)/10+r \\
& *u)-(2*2\text{^}(1/2)*(cot(a)\text{^}2+1)*(cot(a)*(h*r-(7 \\
& *h)/10+r*u))\text{^}(1/2)*(2*h*r-(7*h)/5+2*r*u))/(3 \\
& *cot(a)\text{^}2)+((cot(a)\text{^}2+1)*(2*h*r-(7*h)/5+2*r \\
& *u)*(h*r-(7*h)/10+r*u))/(cot(a)*((2*h*r-(7 \\
& *h)/5+2*r*u)/cot(a))\text{^}(1/2))-(2\text{^}(1/2)*h*(2\text{^}(1/2) \\
& *(cot(a)*(h*r-(7*h)/10+r*u))\text{^}(1/2)-1)*(cot(a)\text{^}2 \\
& +1)*(h*r-(7*h)/10+r*u))/(2*(cot(a)*(h*r-(7 \\
& *h)/10+r*u))\text{^}(1/2))-(2\text{^}(1/2)*h*(2\text{^}(1/2)*(cot(a) \\
& *(h*r-(7*h)/10+r*u))\text{^}(1/2)+1)*(cot(a)\text{^}2+1) \\
& *(h*r-(7*h)/10+r*u))/(2*(cot(a)*(h*r-(7*h)/10 \\
& +r*u))\text{^}(1/2))+(2\text{^}(1/2)*(cot(a)\text{^}2+1)*(2*h*r-(7 \\
& *h)/5+2*r*u)*(h*r-(7*h)/10+r*u))/(3*cot(a) \\
& *(cot(a)*(h*r-(7*h)/10+r*u))\text{^}(1/2))))/(h*(2 \\
& *2\text{^}(1/2)*(cot(a)*(h*r-(7*h)/10+r*u))\text{^}(1/2)-2) \\
& -2\text{^}(1/2)*(2*h-((2*h*r-(7*h)/5+2*r \\
& *u)/cot(a))\text{^}(1/2))*(cot(a)*(h*r-(7*h)/10+r \\
& *u))\text{^}(1/2))-(((2\text{^}(1/2)*(2*h-((2*h*r-(7*h)/5+2 \\
& *r*u)/cot(a))\text{^}(1/2))*(cot(a)\text{^}2+1)*(h*r-(7*h)/10 \\
& +r*u))/(4*(cot(a)*(h*r-(7*h)/10+r*u))\text{^}(1/2)) \\
& -(2\text{^}(1/2)*h*(cot(a)\text{^}2+1)*(h*r-(7*h)/10+r \\
& *u))/(2*(cot(a)*(h*r-(7*h)/10+r*u))\text{^}(1/2)) \\
& +(2\text{^}(1/2)*(cot(a)\text{^}2+1)*(cot(a)*(h*r-(7*h)/10+r \\
& *u))\text{^}(1/2)*(2*h*r-(7*h)/5+2*r*u))/(4*cot(a)\text{^}2 \\
& *((2*h*r-(7*h)/5+2*r*u)/cot(a))\text{^}(1/2)))*(2
\end{aligned}
$$

$$
\begin{aligned}
&* cot(a) * (h - ((2 * h * r - (7 * h)/5 + 2 * r \\
&* u)/cot(a))\text{^}(1/2)) * (h * r - (7 * h)/10 + r * u) - h \\
&* (2\text{^}(1/2) * (cot(a) * (h * r - (7 * h)/10 + r * u))\text{^}(1/2) - 1) \\
&* (2\text{^}(1/2) * (cot(a) * (h * r - (7 * h)/10 + r * u))\text{^}(1/2) + 1) \\
&+ (2 * 2\text{^}(1/2) * (cot(a) * (h * r - (7 * h)/10 + r * u))\text{^}(1/2) \\
&* (2 * h * r - (7 * h)/5 + 2 * r * u))/(3 * cot(a))))/(h * (2 \\
&* 2\text{^}(1/2) * (cot(a) * (h * r - (7 * h)/10 + r * u))\text{^}(1/2) - 2) \\
&- 2\text{^}(1/2) * (2 * h - ((2 * h * r - (7 * h)/5 + 2 * r \\
&* u)/cot(a))\text{^}(1/2)) * (cot(a) * (h * r - (7 * h)/10 + r \\
&* u))\text{^}(1/2)) + ((h * (2\text{^}(1/2) * (cot(a) * (h * r - (7 * h)/10 \\
&+ r * u))\text{^}(1/2) - 1) - (2\text{^}(1/2) * (2 * h - ((2 * h * r - (7 \\
&* h)/5 + 2 * r * u)/cot(a))\text{^}(1/2)) * (cot(a) * (h * r - (7 \\
&* h)/10 + r * u))\text{^}(1/2))/2) * ((2\text{^}(1/2) * (2 * h - ((2 * h * r \\
&- (7 * h)/5 + 2 * r * u)/cot(a))\text{^}(1/2)) * (cot(a)\text{^}2 + 1) * (h \\
&* r - (7 * h)/10 + r * u))/(2 * (cot(a) * (h * r - (7 * h)/10 + r \\
&* u))\text{^}(1/2)) - (2\text{^}(1/2) * h * (cot(a)\text{^}2 + 1) * (h * r - (7 \\
&* h)/10 + r * u))/(cot(a) * (h * r - (7 * h)/10 + r * u))\text{^}(1/2) \\
&+ (2\text{^}(1/2) * (cot(a)\text{^}2 + 1) * (cot(a) * (h * r - (7 * h)/10 + r \\
&* u))\text{^}(1/2) * (2 * h * r - (7 * h)/5 + 2 * r * u))/(2 * cot(a)\text{^}2 \\
&* ((2 * h * r - (7 * h)/5 + 2 * r * u)/cot(a))\text{^}(1/2))) * (2 \\
&* cot(a) * (h - ((2 * h * r - (7 * h)/5 + 2 * r \\
&* u)/cot(a))\text{^}(1/2)) * (h * r - (7 * h)/10 + r * u) - h \\
&* (2\text{^}(1/2) * (cot(a) * (h * r - (7 * h)/10 + r * u))\text{^}(1/2) - 1) \\
&* (2\text{^}(1/2) * (cot(a) * (h * r - (7 * h)/10 + r * u))\text{^}(1/2) + 1) \\
&+ (2 * 2\text{^}(1/2) * (cot(a) * (h * r - (7 * h)/10 + r * u))\text{^}(1/2) \\
&* (2 * h * r - (7 * h)/5 + 2 * r * u))/(3 * cot(a))))/(h * (2 \\
&* 2\text{^}(1/2) * (cot(a) * (h * r - (7 * h)/10 + r * u))\text{^}(1/2) - 2) \\
&- 2\text{^}(1/2) * (2 * h - ((2 * h * r - (7 * h)/5 + 2 * r \\
&* u)/cot(a))\text{^}(1/2)) * (cot(a) * (h * r - (7 * h)/10 + r \\
&* u))\text{^}(1/2))\text{^}2
\end{aligned}
$$

$$Eu = r*u - (((2\text{^}(1/2)*r*(cot(a)*(h*r - (7*h)/10 + r*u))\text{^}(1/2))/(2*cot(a)*((2*h*r - (7*h)/5 + 2*r*u)/cot(a))\text{^}(1/2)) - (2\text{^}(1/2)*r*cot(a)*(2*h - ((2*h*r - (7*h)/5 + 2*r*u)/cot(a))\text{^}(1/2)))/(4*(cot(a)*(h*r - (7*h)/10 + r*u))\text{^}(1/2)) + (2\text{^}(1/2)*h*r*cot(a))/(2*(cot(a)*(h*r - (7*h)/10 + r*u))\text{^}(1/2)))*(2*cot(a)*(h - ((2*h*r - (7*h)/5 + 2*r*u)/cot(a))\text{^}(1/2))*(h*r - (7*h)/10 + r*u) - h*(2\text{^}(1/2)*(cot(a)*(h*r - (7*h)/10 + r*u))\text{^}(1/2) - 1)*(2\text{^}(1/2)*(cot(a)*(h*r - (7*h)/10 + r*u))\text{^}(1/2) + 1) + (2*2\text{^}(1/2)*(cot(a)*(h*r - (7*h)/10 + r*u))\text{^}(1/2)*(2*h*r - (7*h)/5 + 2*r*u))/(3*cot(a))))/(h*(2*2\text{^}(1/2)*(cot(a)*(h*r - (7*h)/10 + r*u))\text{^}(1/2) - 2) - 2\text{^}(1/2)*(2*h - ((2*h*r - (7*h)/5 + 2*r*u)/cot(a))\text{^}(1/2))*(cot(a)*(h*r - (7*h)/10 + r*u))\text{^}(1/2)) + ((h*(2\text{^}(1/2)*(cot(a)*(h*r - (7*h)/10 + r*u))\text{^}(1/2) - 1) - (2\text{^}(1/2)*(2*h - ((2*h*r - (7*h)/5 + 2*r*u)/cot(a))\text{^}(1/2))*(cot(a)*(h*r - (7*h)/10 + r*u))\text{^}(1/2))/2)*((2*r*(h*r - (7*h)/10 + r*u))/((2*h*r - (7*h)/5 + 2*r*u)/cot(a))\text{^}(1/2) - 2*r*cot(a)*(h - ((2*h*r - (7*h)/5 + 2*r*u)/cot(a))\text{^}(1/2)) - (2\text{^}(1/2)*r*(2*h*r - (7*h)/5 + 2*r*u))/(3*(cot(a)*(h*r - (7*h)/10 + r*u))\text{^}(1/2)) - (4*2\text{^}(1/2)*r*(cot(a)*(h*r - (7*h)/10 + r*u))\text{^}(1/2))/(3*cot(a)) + (2\text{^}(1/2)*h*r*cot(a)*(2\text{^}(1/2)*(cot(a)*(h*r - (7*h)/10 + r*u))\text{^}(1/2) - 1))/(2*(cot(a)*(h*r - (7*h)/10 + r*u))\text{^}(1/2)) + (2\text{^}(1/2)*h*r*cot(a)*(2\text{^}(1/2)*(cot(a)*(h*r - (7*h)/10 + r*u))\text{^}(1/2) + 1))/(2*(cot(a)*(h*r - (7*h)/10 + r*u))\text{^}(1/2))))/(h*(2*2\text{^}(1/2)*(cot(a)*(h*r - (7*h)/10$$

$$+ r*u))\text{^}(1/2) - 2) - 2\text{^}(1/2)*(2*h - ((2*h*r - (7*h)/5 + 2*r*u)/cot(a))\text{^}(1/2))*(cot(a)*(h*r - (7*h)/10 + r*u))\text{^}(1/2)) + ((h*(2\text{^}(1/2)*(cot(a)*(h*r - (7*h)/10 + r*u))\text{^}(1/2) - 1) - (2\text{^}(1/2)*(2*h - ((2*h*r - (7*h)/5 + 2*r*u)/cot(a))\text{^}(1/2))*(cot(a)*(h*r - (7*h)/10 + r*u))\text{^}(1/2))/2)*((2\text{^}(1/2)*r*(cot(a)*(h*r - (7*h)/10 + r*u))\text{^}(1/2))/(cot(a)*((2*h*r - (7*h)/5 + 2*r*u)/cot(a))\text{^}(1/2)) - (2\text{^}(1/2)*r*cot(a)*(2*h - ((2*h*r - (7*h)/5 + 2*r*u)/cot(a))\text{^}(1/2)))/(2*(cot(a)*(h*r - (7*h)/10 + r*u))\text{^}(1/2)) + (2\text{^}(1/2)*h*r*cot(a))/(cot(a)*(h*r - (7*h)/10 + r*u))\text{^}(1/2))*(2*cot(a)*(h - ((2*h*r - (7*h)/5 + 2*r*u)/cot(a))\text{^}(1/2))*(h*r - (7*h)/10 + r*u) - h*(2\text{^}(1/2)*(cot(a)*(h*r - (7*h)/10 + r*u))\text{^}(1/2) - 1)*(2\text{^}(1/2)*(cot(a)*(h*r - (7*h)/10 + r*u))\text{^}(1/2) + 1) + (2*2\text{^}(1/2)*(cot(a)*(h*r - (7*h)/10 + r*u))\text{^}(1/2)*(2*h*r - (7*h)/5 + 2*r*u))/(3*cot(a))))/(h*(2*2\text{^}(1/2)*(cot(a)*(h*r - (7*h)/10 + r*u))\text{^}(1/2) - 2) - 2\text{^}(1/2)*(2*h - ((2*h*r - (7*h)/5 + 2*r*u)/cot(a))\text{^}(1/2))*(cot(a)*(h*r - (7*h)/10 + r*u))\text{^}(1/2))\text{^}2$$

In the above equations, we have considered the breadth of the prism equal to 1 (b=1). We have yet to determine the ratio of densities (r) and the height of the prism (h) in order to find the unknown values (a, u). By changing the values of r,h, we can estimate the domain of definition of a, u.

The process of determining the above domains of definition consists of the following steps:

- Definition of the factors r,h
- Creation of a system 2 x 2 for each case
- Comprehension of the domain of definition for each case
- Creation of a MatLab code that solves the system
- Solution of the system
- Comprehension of the factors that can affect these solutions
- Creation of a MatLab code that plots the amount of the solutions in relation to these factors
- Surpass any technical difficulties in plotting with MatLab
- Understanding and analyzing the resulting diagrams
- Confirmation of the results by implementing experiments

6.0 Theoretical background in nonlinear dynamics

Before we discuss the resulting diagrams, it is crucial to understand the principles of non linear dynamics. This is the subject that deals with change and more specifically systems that evolve over time. We use no linear dynamics in order to analyze the behavior of a system, whether the system in question settles down to equilibrium, keeps repeating in time or does something more complicated. In particular, we have to explain the theory of two- dimensional flow which is very close to our case.

6.1Fixed points and stability

Let's consider a non-linear, one dimension, differential equation $\dot{x} = f(x)$. We imagine that a fluid is flowing along the real line with a local velocity f(x). This imaginary fluid is called the phase fluid and the real line is the phase space. The flow is to the right where f(x) >0 and to the left where f(x) <0. To find the solution to $\dot{x} = f(x)$starting from an arbitrary initial condition x_0, we place an imaginary point (known as phase point) at x_0 and watch how it is carried along by the flow. As time goes on, the phase point moves along the x- axis according to some function x(t). This function is called the trajectory based at x_0, and it represents the solution of the differential equation starting from the initial condition x_0. A picture like Fig. 16, which shows all the qualitatively different trajectories of the system, is called a phase portrait. The appearance of a phase portrait is called by the fixed points x^*, defined by $f(x^*)=0$; they correspond to stagnation points of the flow. The solid black dots correspond to stable fixed points (the local flow is toward it) and the open dots correspond to unstable fixed points (the flow is away from it). In Fig. 16 we can see a stable fixed point. In terms of the original differential equation, fixed points represent equilibrium solutions (sometimes called steady, constant or rest solutions, since, if $x=x^*$ then $x(t)=x^*$ for all time). Equilibrium is defined to be stable if all sufficiently small disturbances away from it dump out in time. Thus stable equilibrium is represented geometrically by stable fixed points. Conversely, unstable equilibrium, in which disturbances grow in time, is represented by unstable fixed points.

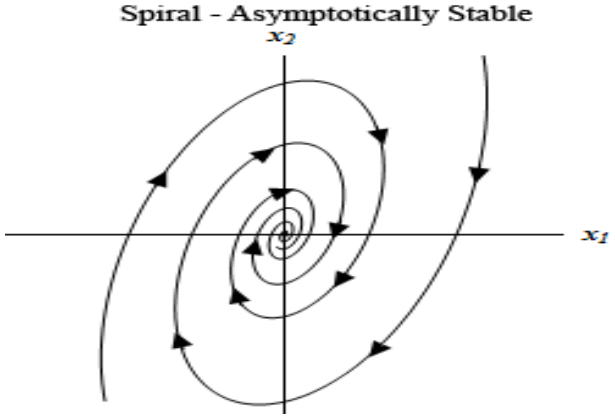

Figure 15: Phase portrait [23]

6.2 Bifurcations

6.2.1 Introduction

The dynamics of vector field is very limited: all solutions either settle down to equilibrium or head out to$\pm\infty$. However, we can also see a dependence on parameters. The qualitative structure of the flow can change as parameters are varied. In particular, fixed points can be created or destroyed, or their stability can change. These qualitative changes in the dynamics are called bifurcations, and the parameter values at which they occur are called bifurcations points. Bifurcations are important scientifically- they provide models of transitions and instabilities as some control parameter is varied. The important categories of bifurcations are saddle-node, transcritical and Pitchfork bifurcations. The last one is the kind we mainly deal with in our thesis so, we are going to analyze its theoretical basis extensively. After that, there is a brief analysis of saddle-node bifurcations.

6.2.2 Pitchfork bifurcation [24]

This bifurcation is common in physical problems that have symmetry. For example, many problems have a spatial symmetry between left and right. In such cases, fixed points tend to appear and disappear in symmetrical pairs. There are two very different types of Pitchfork bifurcations. The simpler type is called supercritical and will be discussed first.

Supercritical Pitchfork Bifurcation

The normal form of the supercritical Pitchfork bifurcation is:

$$\dot{x} = rx - x^3$$

As we can see, this equation is invariant under the change of variable $x \rightarrow -x$. That is, if we replace x by –x and then cancel the resulting minus signs on both sides of the equation, we get the first equation back again. This invariance is the mathematical expression of the left-right symmetry mentioned earlier. As we see in Fig. 27, when r<0, the origin is the only fixed point, and it is stable. When r=0, the origin is still stable, but much more weakly so, since the linearization vanishes. Now solutions no longer decay exponentially fast- instead the decay is a much slower algebraic function of time. Finally, when r>0, the origin has become unstable. Two new stable fixed points appear on either side of the origin, symmetrically located at $x^* = \pm\sqrt{r}$.

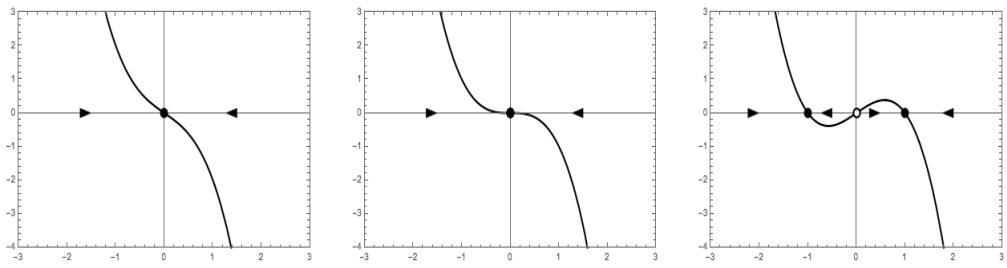

Figure 16: Supercritical Pitchfork Bifurcation for varied values of r. [25]

The reason for the term pitchfork becomes clear when we plot the bifurcation diagram.

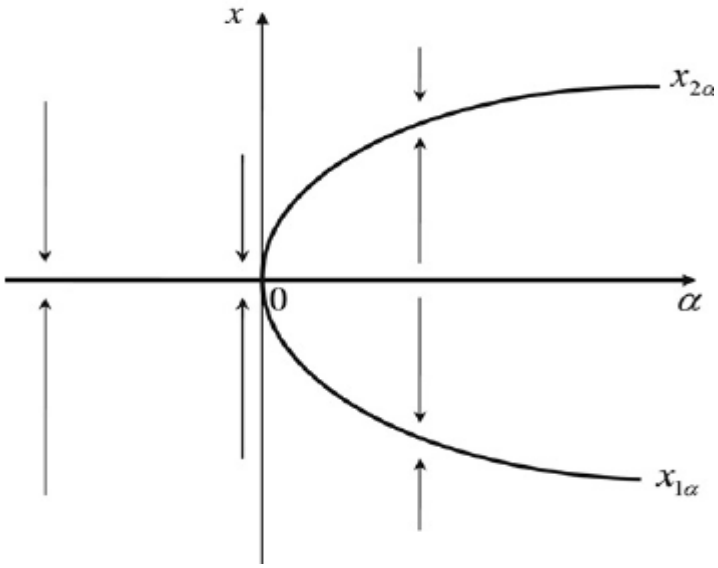

Figure 17: Supercritical Pitchfork bifurcation diagram. [25]

Subcritical Pitchfork Bifurcation

In the supercritical case discussed above, the cubic term is stabilizing; it acts as a restoring force that pulls x(t) back toward x=0. If instead the cubic term were destabilizing, then, we would have a subcritical Pitchfork bifurcation:

$$\dot{x} = rx + x^3$$

Compared to the supercritical bifurcation diagram, the subcritical diagram is inverted. The nonzero fixed points $x^* = \pm\sqrt{-r}$ are unstable, and exist only below the bifurcation (r<0), which motivates the term 'subcritical'. More importantly, the origin is stable for r<0 and unstable for r>0, as in the supercritical case, but now the instability for r>0 is not opposed by the cubic term- in fact the cubic term lends a

helping hand in driving the trajectories out to infinity. This effect leads to blow-up ($x(t) \rightarrow \pm\infty$ in finite time, starting from any initial condition $x_0 \neq 0$).

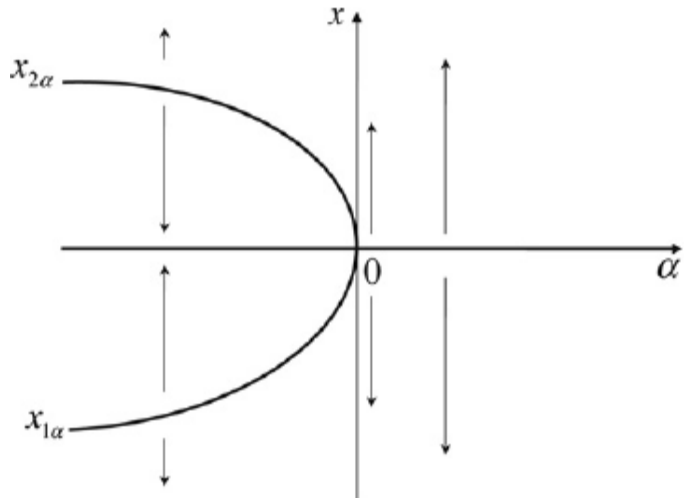

Figure 18: Subcritical Pitchfork bifurcation diagram. [25]

In real physical systems, such an explosive instability is usually opposed by the stabilizing influence of higher-order terms. Assuming that the system is still symmetrical under $x \rightarrow -x$, the first stabilizing term must be x^5. Thus the canonical example of a system with a subcritical pitchfork bifurcation is:

$$\dot{x} = rx + x^3 - x^5$$

There is no loss in generality in assuming that the coefficients of x^3 and x^5 are 1.

6.2.3 Saddle-node bifurcation [24]

The saddle-node bifurcation is the basic mechanism by which fixed points are created and destroyed. As a parameter is varied, two fixed points move toward each other, collide and mutually annihilate. The prototypical example of a saddle-node bifurcation is given by the first order system:

$$\dot{x} = r + x^2$$

where r is the parameter, which may be positive, negative or zero. When r is negative, there are two fixed points, one stable and one unstable. As r approaches 0 from below, the parabola moves up and the two fixed points move toward each other. When r=0, the fixed points coalesce into a half-stable fixed point at $x^*=0$. This type of fixed point is extremely delicate- it vanishes as soon as r>0, and now there are no fixed points at all. In this example, we say that a bifurcation occurred at r=0, since the vector fields for r>0 and r<0 are qualitatively different.

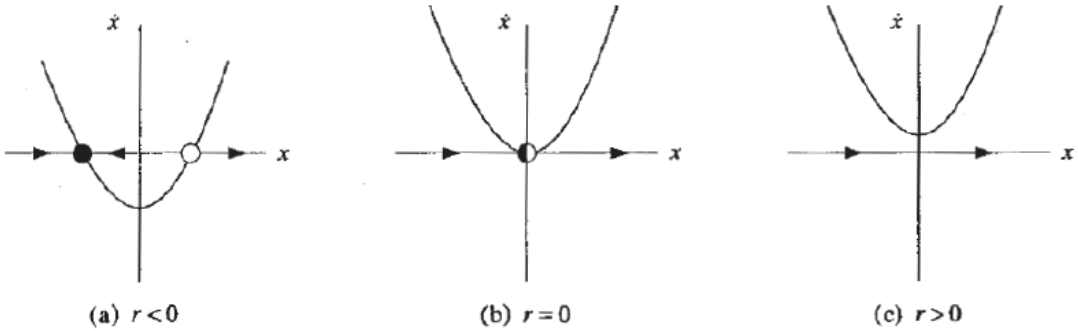

Figure 19: Saddle-node bifurcation as r is varied. [25]

6.2.4Imperfect bifurcations [24]

Let's consider a perturbed, or imperfect, pitchfork bifurcation that is described by the equation:

$$x_t = \lambda + \mu x - x^3$$

where (λ,μ) $\in R^2$ are real parameters. Note that if λ = 0, this system has the reflectional symmetry x → −x and a Pirchfork bifurcation, but this symmetry is broken when λ ≠0.

There are three real roots if μ > 0 and$27\lambda^2 < 4\mu^3$, and one real root if $27\lambda^2 > 4\mu^3$. The surface of the roots as a function of (λ,μ) forms a cusp catastrophe. If λ ≠0, the pitchfork bifurcation is perturbed to a stable branch that exists for all values of μ without any bifurcations and a supercritical saddle-node bifurcation in which the remaining stable and unstable branches appear.

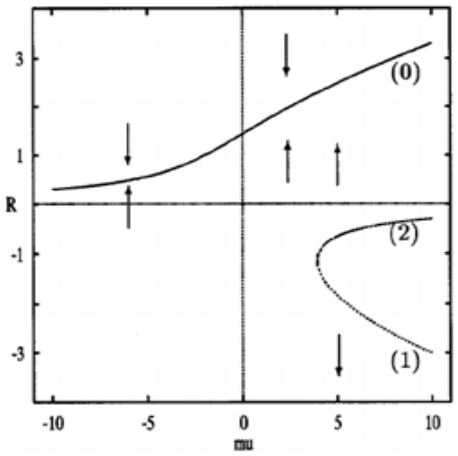

Figure 20: Imperfect Bifurcation diagram [25]

7.0 Results of the energy method

In this chapter, we present the results of the MatLab code for a prism with internal liquid. We chose to present our results in diagrams that show how the heeling angle (a) changes value in relation to different factors, such as the height of the internal liquid (a) or the ratio of densities (r). By examining the resulting diagrams we can clearly see that the bifurcation phenomenon takes place. Understanding the last chapter is advised for a better comprehension of these diagrams.

7.1Diagrams presentation

To start with, we present the diagrams a-u as they were created by MatLab and the energy approach. We modify the parameter u- height of the internal liquid and we observe how the parameter a- angle of heel of the prism is affected. The constant line shows the stable balance positions of the system while the broken line shows the unstable ones. We start with the diagrams of a symmetric, square prism (λ=1) and we continue with the same diagrams for an orthogonal prism (λ<1).

Symmetric prismλ=1

- W=2.5 kg

r=1

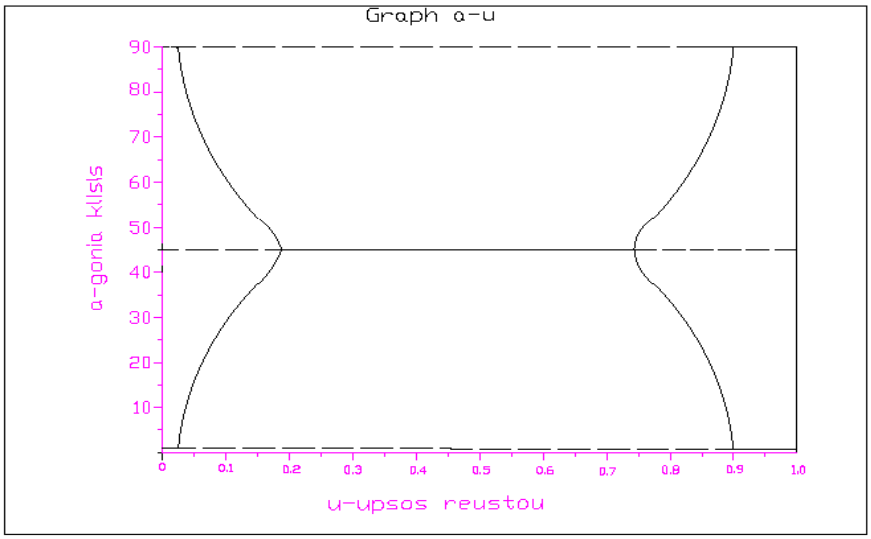

Figure 21: Diagram a-u for a square prism.

r=0.9

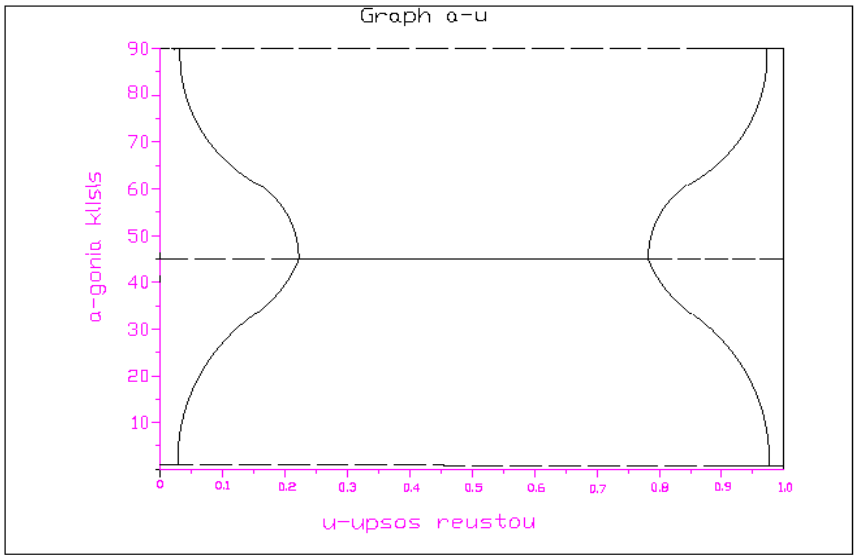
Graph a-u
a-gonia klisis
90
80
70
60
50
40
30
20
10
0
0.1
0.2
0.3
0.4
0.5
0.6
0.7
0.8
0.9
1.0
u-upsos reustou

r=0.7

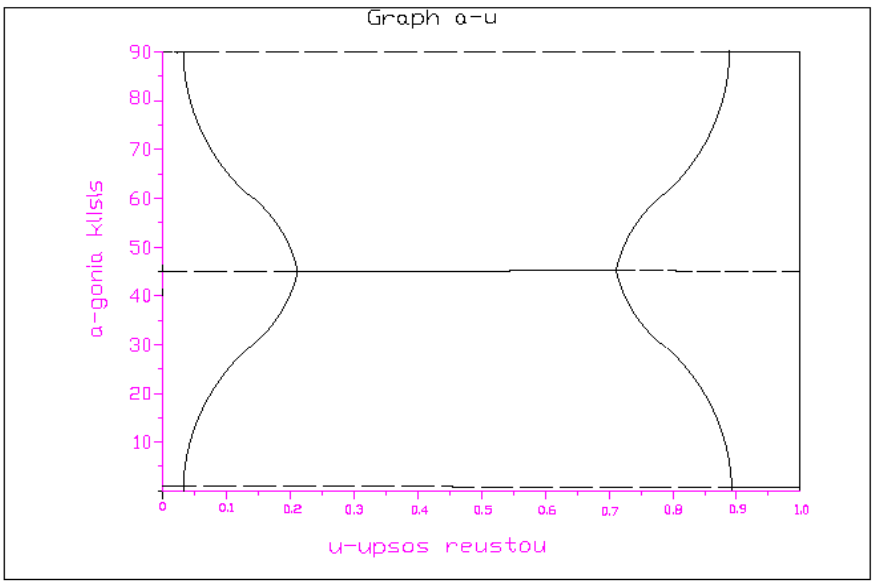
Graph a-u
a-gonia klisis
90
80
70
60
50
40
30
20
10
0
0.1
0.2
0.3
0.4
0.5
0.6
0.7
0.8
0.9
1.0
u-upsos reustou

r=0.5

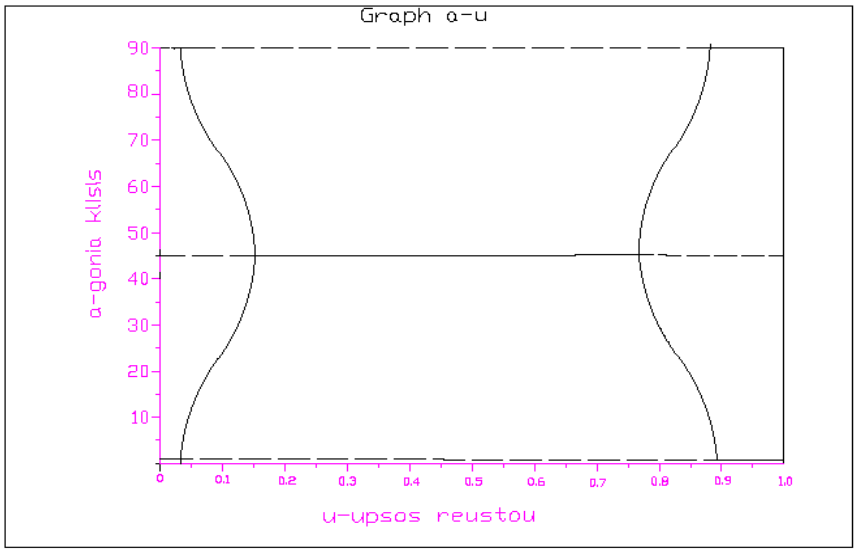
Graph a-u
a-gonia klisis
90
80
70
60
50
40
30
20
10
0
0.1
0.2
0.3
0.4
0.5
0.6
0.7
0.8
0.9
1.0
u-upsos reustou

r=0.3

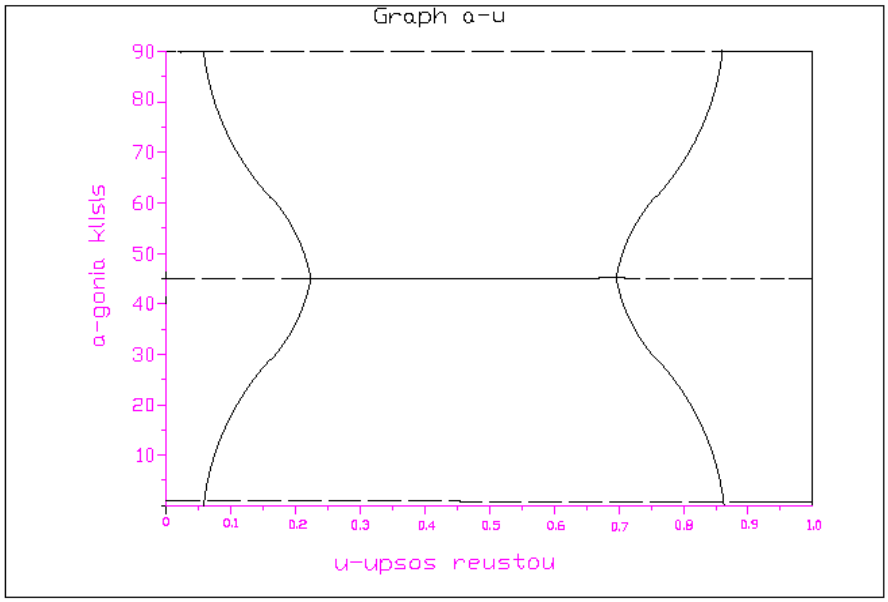
Graph a-u
a-gonia klisis
90
80
70
60
50
40
30
20
10
0
0.1
0.2
0.3
0.4
0.5
0.6
0.7
0.8
0.9
1.0
u-upsos reustou

r=0.1

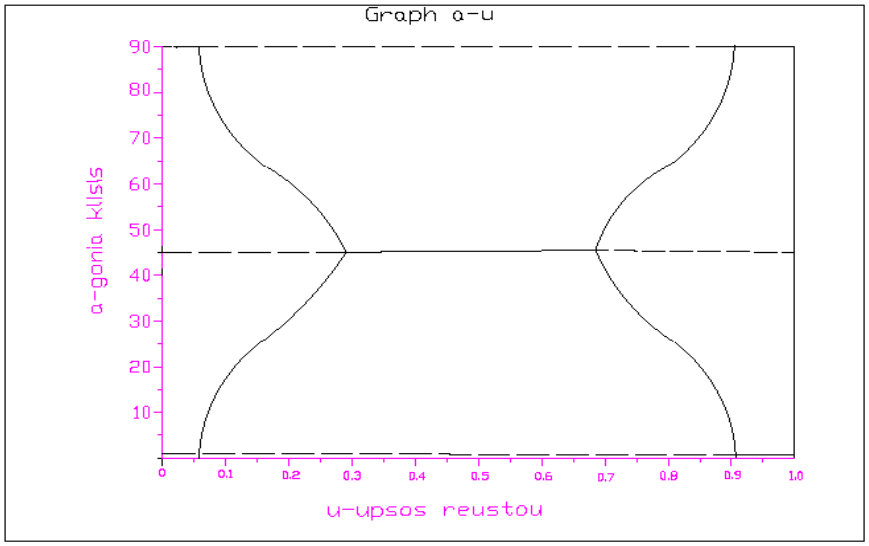

Figure 22: Diagrams a-u for a square prism in different r

Diagram a-r for u=0.3

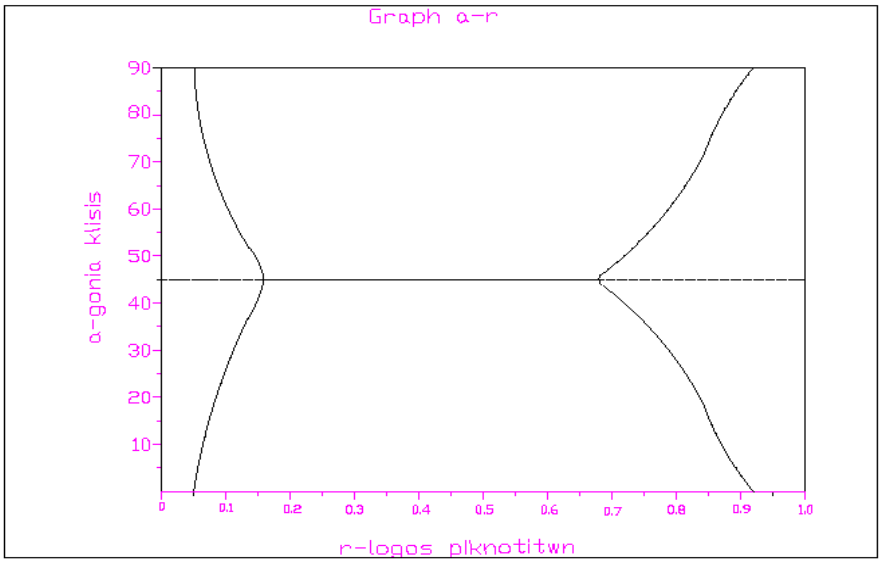

Figure 23: Diagram a-r for a square prism and u=0.3

Diagram a-u for r=1.0

- W=1.5 kg

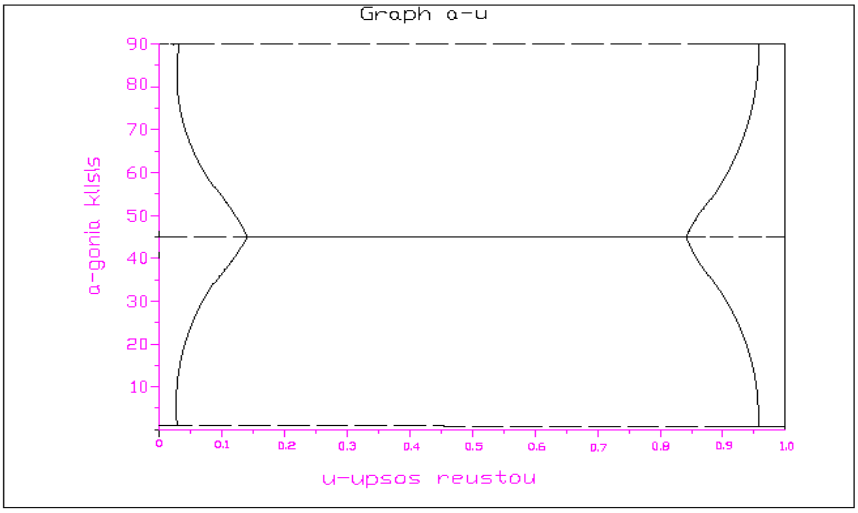

- W=2.0kg

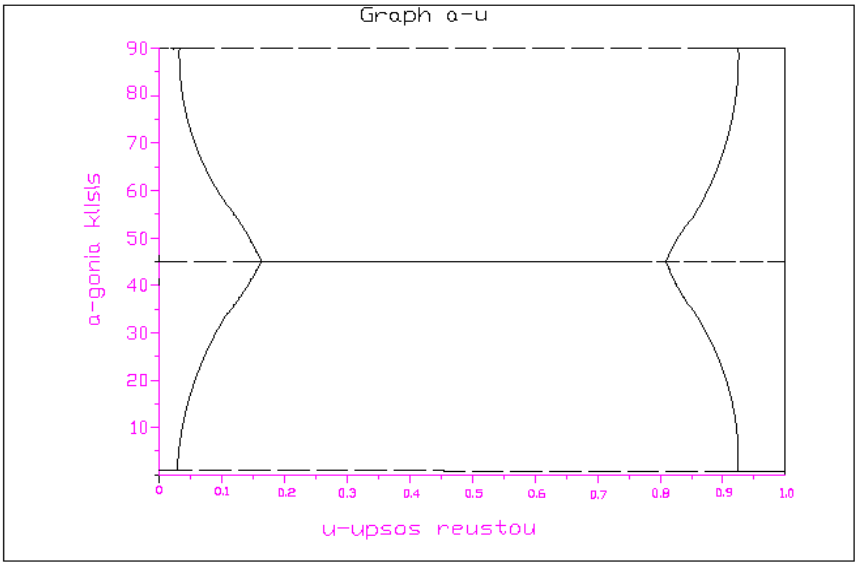

- W=2.5kg

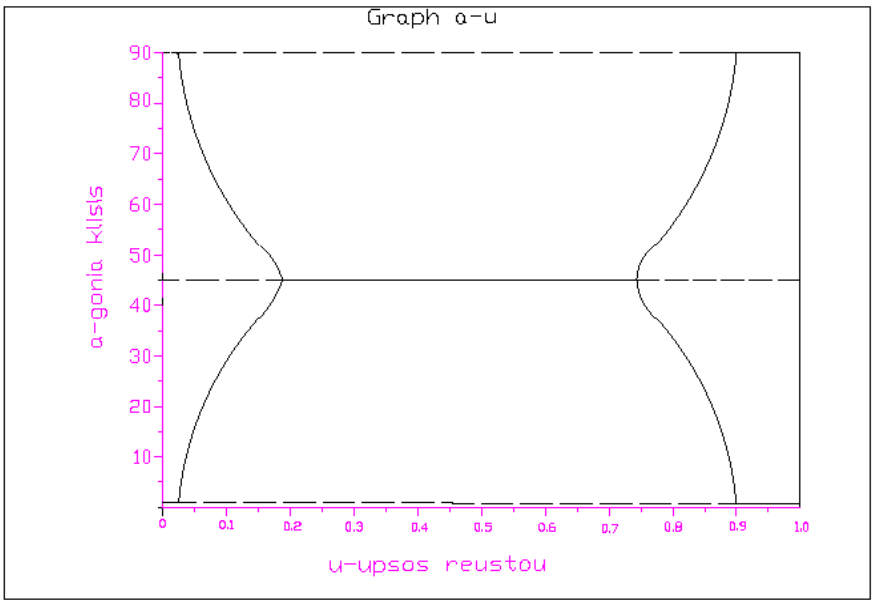

- W=3.0kg

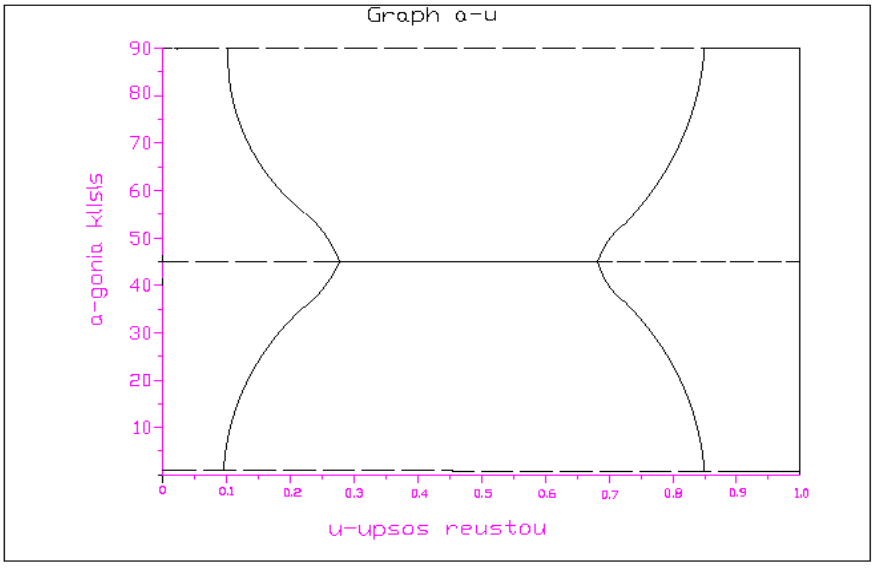

Figure 24: Diagram a-u for a square prism and varied weight of void prism

Varying the ratio λ

λ=0.99

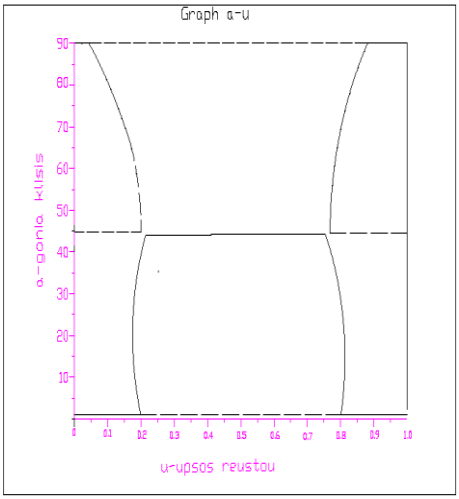

λ=0.98

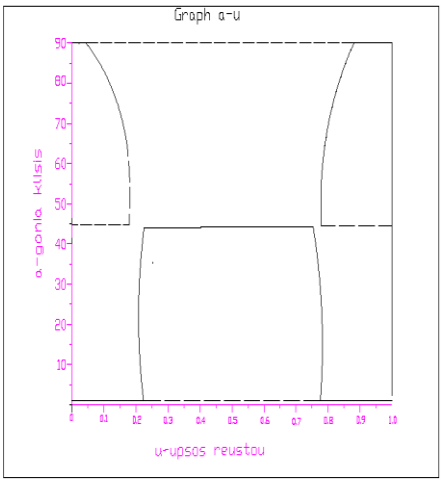

λ=0.97

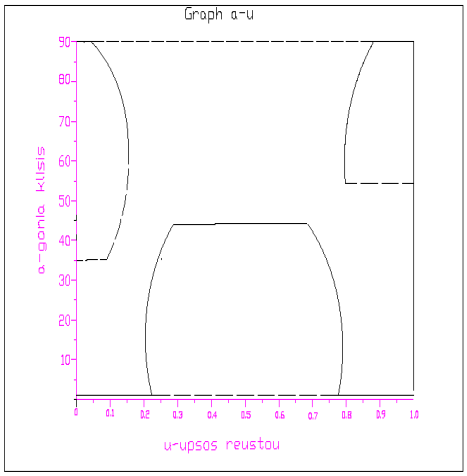

λ=0.90

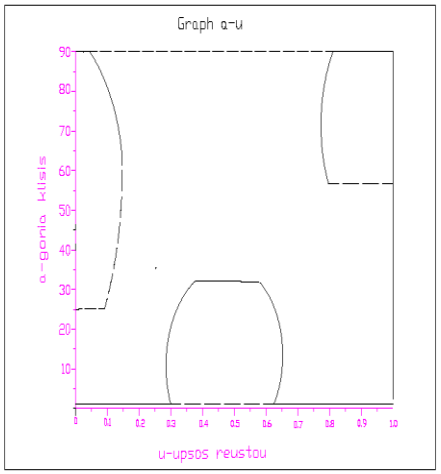

λ=0.85 λ=0.82

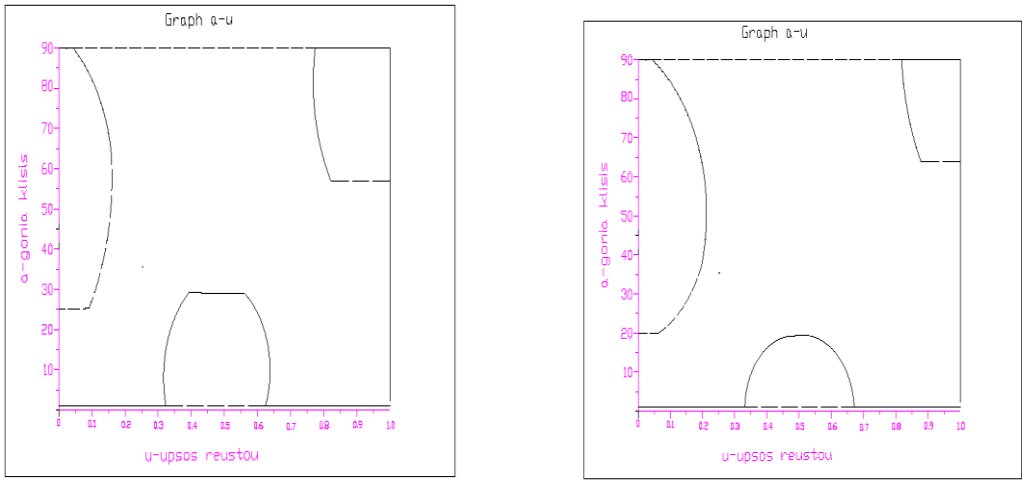

Figure 25: Diagram a-u for orthogonal prism with varying λ.

Orthogonal prism λ=0.8

- W=2.5kg

r=1.0

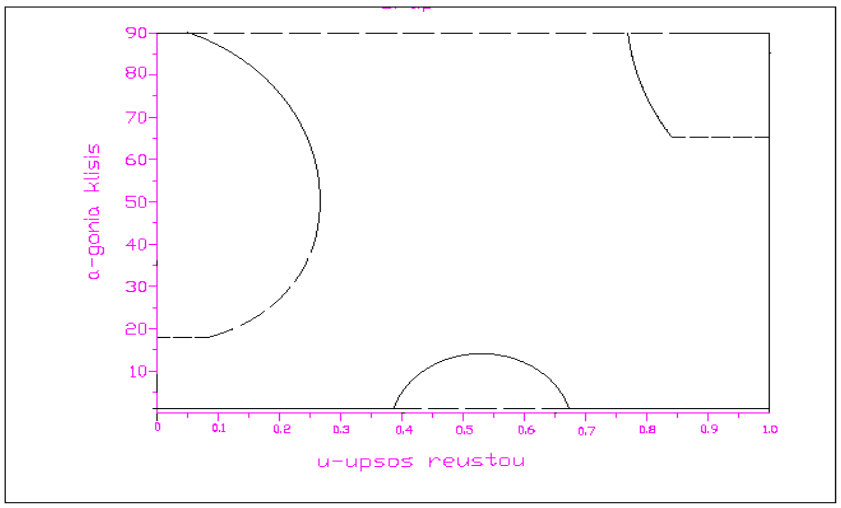

Figure 26: Diagram a-u for an orthogonal prism.

r=0.7

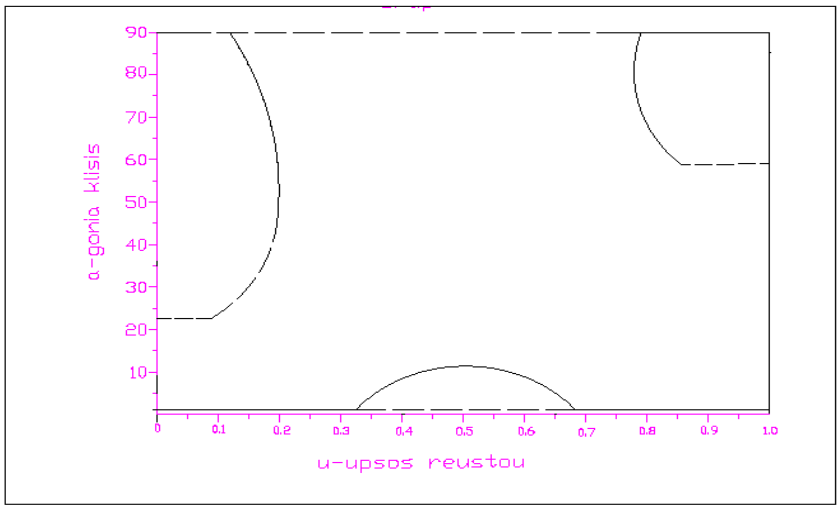
90
80
70
60
50
40
30
20
10
a-gonia klisis
0
0.1
0.2
0.3
0.4
0.5
0.6
0.7
0.8
0.9
1.0
u-upsos reustou

r=0.5

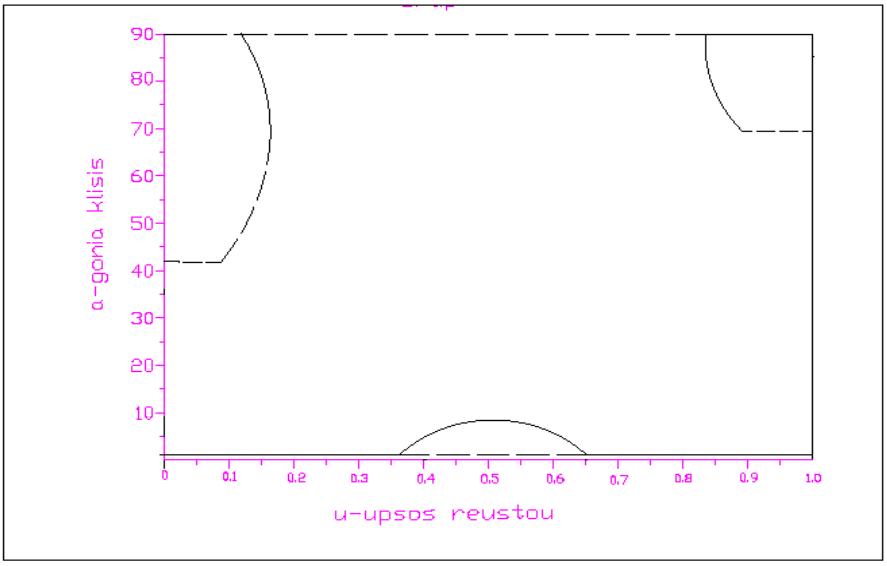
90
80
70
60
50
40
30
20
10
a-gonia klisis
0
0.1
0.2
0.3
0.4
0.5
0.6
0.7
0.8
0.9
1.0
u-upsos reustou

r=0.3

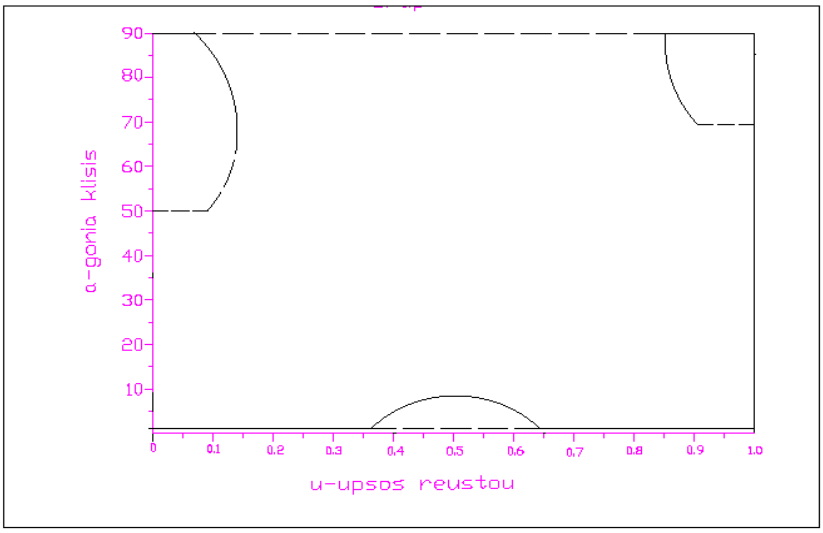

r=0.1

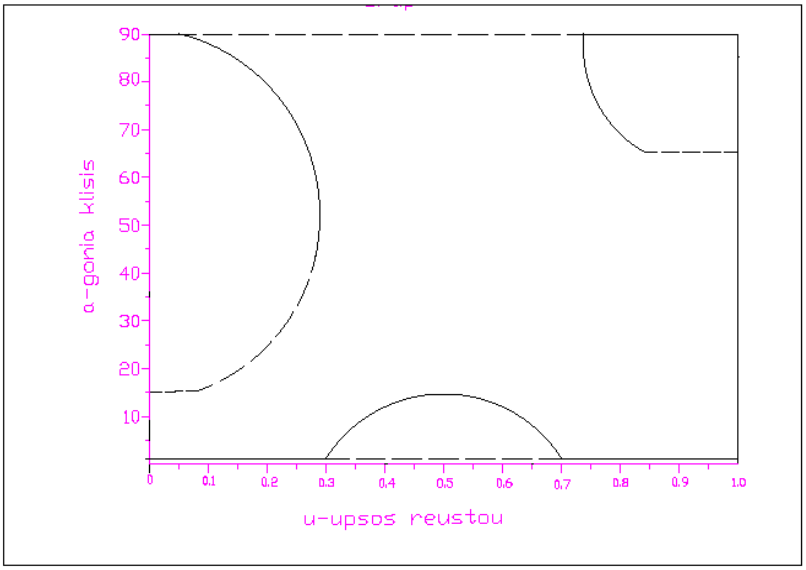

Figure 27: Diagrams a-u for an orthogonal prism for varied r.

Diagram a-u for λ=0.8

- W=1.5kg

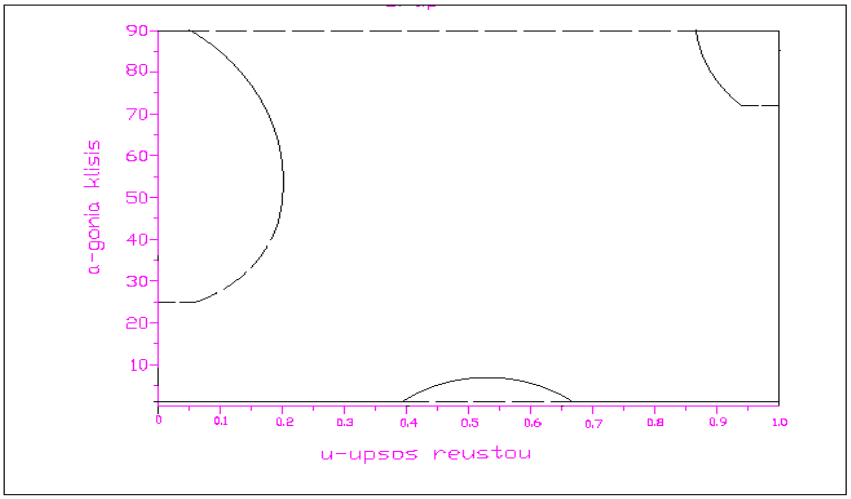

- W=2.0kg

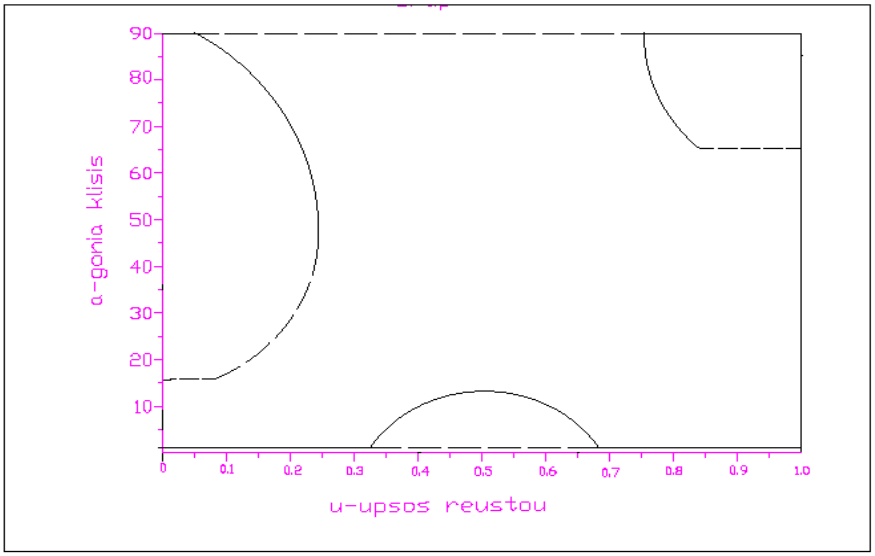

- W=2.5kg

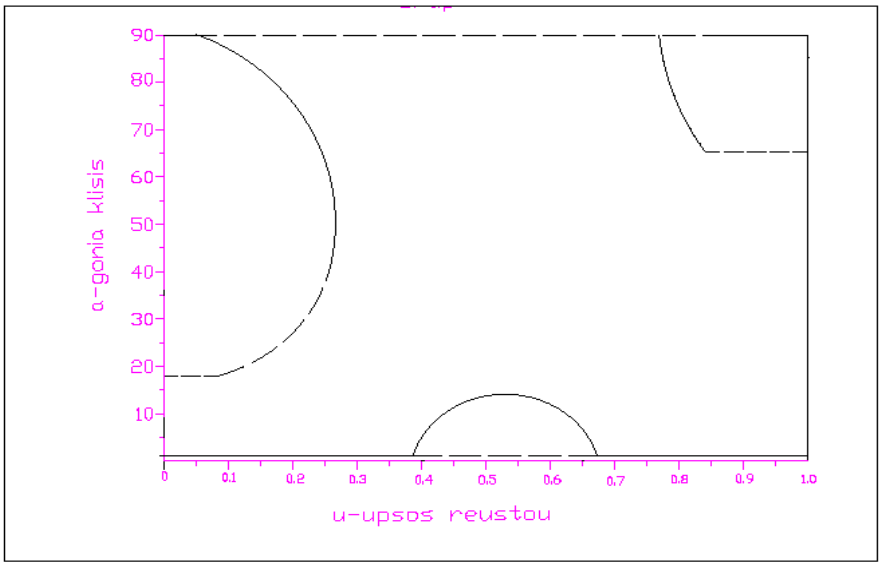

- W=3.0kg

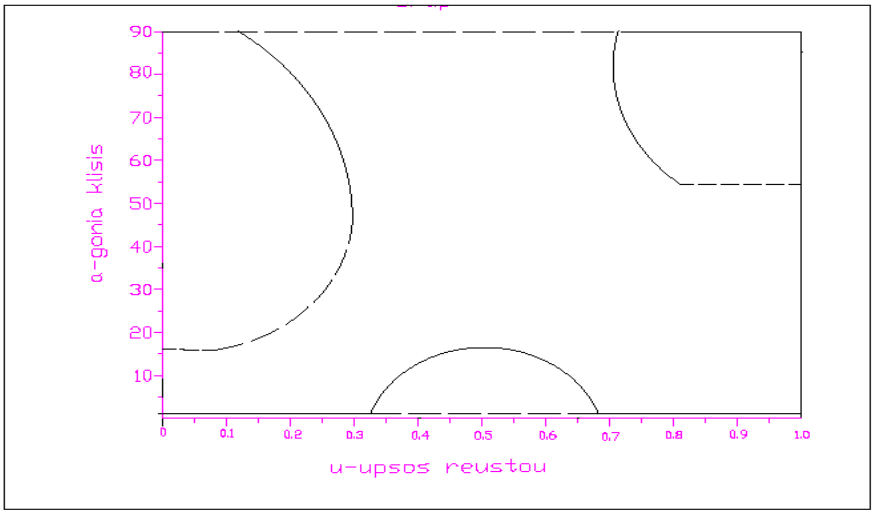

Figure 28: Diagrams a-u for an orthogonal prism for v

7.2 Conclusions

- When a body is characterized by symmetry, we observe this symmetry in the diagrams as well. The symmetry concerns both the horizontal and the vertical axis. In some cases, the symmetry is not perfect but we will discuss some possible reasons below.
- In the diagrams of the symmetrical case, we recognize the creation of two supercritical Pitchfork bifurcations. In reality, we can safely assume that this symmetry is presented in any pi/2 rad. If we expand the vertical axis, we will see the symmetry to be repeated.
- We should also focus in the interval between u=0.15 and u=0.20. In that interval, we observe the famous symmetry breaking. That means that the floating body has the ability to balance at non symmetrical positions as well. In the rest of the values of u, the body balances to either stable or unstable symmetrical positions.
- It is interesting to note the alternation of the stable to the unstable positions and backwards. It is exactly like the buckling example.
- When we modify r parameter, we observe an interesting phenomenon as well. For extremely high and low values of r, the prism mainly balances at symmetrical positions. For intermediate values of r, the prism has the ability to balance at non symmetrical positions for more values of u.
- We should also observe the differences between the diagrams of the orthogonal and the square prism. There is loss of the symmetry in the vertical axis whilst the symmetry in the horizontal axis is maintained for small values of r. The basic cause is the change of the centre of gravity. As a result, we can understand the importance of the factor λ. The KG (centre of gravity) factor is mostly affected by the external casing. Contrary to the case of a solid internal material that is adjusted to the casing and does not move into the prism, the internal liquid is independent enough of the KG factor. Consequently, the heavier the prism is, the stronger the KG factor is.
- The way the factor r affects the values of a remains the same. We observe that in big and small values of r, the symmetry breaking delays more.
- Another important factor is the weight of the prim. The symmetry breaking appears earlier in lighter prisms. This is a logical and expectable phenomenon. The lighter the prism is, the easier the angle of heel is created. So, when the prism is heavy, it can maintain its starting balance position for higher values of u.

8.0 Experimental approach of stability

Main target of the experiments was the confirmation of the theoretical results. The lack of theoretical background and scientific sources on the issue created this need. Our goal was to recreate some of the above diagrams by using the results of the experimental measurements. The finite number of measurements does not allow us to create diagrams of same quality but they are adequate enough to make some satisfactory conclusions.

8.1 Experimental arrangement

The experimental procedure took place in the laboratory of Nautical and Marine Hydrodynamics of the faculty. The experimental equipment we used was:

1. **Prismatic models**

We used two prismatic models of different dimensions. In particular, we chose two prisms, an orthogonal (λ=1) and a square one (λ=0.9), of small enough dimensions in order to fit in the tank. In the previous chapter, we considered a prism of infinite length. In order to approach this, the prism used in the experiment had the third dimension (length of the prism) much bigger than the other two. The dimensions of the prisms were:

- **Orthogonal prism: 20x18x50 cm (t=0.5cm)**
- **Square prism: 20x20x50 cm (t=0.5cm)**

As we have already mentioned, the prisms were hollow in order to fill them with different liquids. In the middle of the prism, there was a small circular aperture of d=3cm that was needed to flood the model with liquid. After that, we used a cap to close the aperture and sink the model into the tank. The cap was of Plexiglass as was the rest of the model. Plexiglas is a transparent, waterproof and light material, ideal for this experiment.

2. **Internal liquid**

The initial idea was to use many different materials of diverse specific gravity (r). In this way, we could test more cases. However, trying to find an easily manageable and harmless liquid, we confronted some difficulties. So, we ended up choosing pure water.

3. **External liquid**

The external tank contained pure water as well. In order to simplify the problem, we consider mass density of the water ρ=1g/cm^3, regardless the external temperature. The basic factor of the problem is the value of the ratio r (r=$\frac{mass\ density\ of\ the\ external\ liquid}{mass\ density\ of\ the\ internal\ liquid}$). Choosing pure water as both the internal and external liquid makes the ratio of densities equal to one. This fact particularizes our

case but we can safely consider that our results can be generalized. If our results are correct for this case, our approach is correct.

4. **External tank**

The tank was made out of Plexiglas. Its basic internal dimensions were 40x40x60 cm.

5. **Further auxiliary equipment**

A precise scale 10g was used in order to weigh the prism both full and empty. A metric film was also used in order to measure the dimensions of the prisms into the tank.

It is important to mention that any measuring error was ignored when processing the experimental results. This kind of errors were neglected in order to simplify the process.

8.2 Experimental procedure

We started with the measurement of the dimensions and the weighing of the prisms. Precision was at the most importance during this procedure as the special weight of the material is a factor of our equations.

During the experiment, we followed the steps below:

- We filled the tank with pure water.
- We stuck the metric films onto the prism using tape.
- We flooded the first prism with some water.
- We measured the height of the internal water.
- We consulted our theoretical results to find out the unstable balance positions.
- We sunk the prism into the tank.
- We observed the prism to see its comportment to the prospective unstable balance position.
- We waited for it to balance.
- We measured the heel of angle.
- We repeated for different heights of internal water.
- We repeated for the second prism.

For each height of internal water, a prism has one or more unstable balance positions. However, during the experiment we cannot find them because the body only balances to stable ones by itself. The only way to find the unstable balance positions was to check whether the body stands on this position for some seconds. In order to observe such a quick movement, we should know this position beforehand. So, before the placement of the prism inside the tank, we were consulting the theoretical results.

8.3 Experimental results

We firstly calculated the prisms' densities:

Models	$m(g)$	$V\,(cm^3)$	$\rho(g/cm^3)$
Square prism (λ= 1)	2640	2311	1.142
Orthogonal prism (λ= 0.9)	2460	2173	1.132
ρ	-	-	1.137

Figure 29: Mass density of the prisms

The volume that occupies the material of the prisms was calculated by the equation below:

$$V = Vout - Vin = b \times h \times l - (b - 2t) \times (h - 2t) \times (l - 2t)$$

Mass density of Plexiglas: $\rho = \frac{m}{V}$

Average value of the mass density of Plexiglas: $\rho = \frac{\rho_{\lambda=1} + \rho_{\lambda=0.9}}{2}$

Now, we are going to present the rest of the experimental measurements in an aggregate table. In order to clarify the values measured, we adduce the following figure:

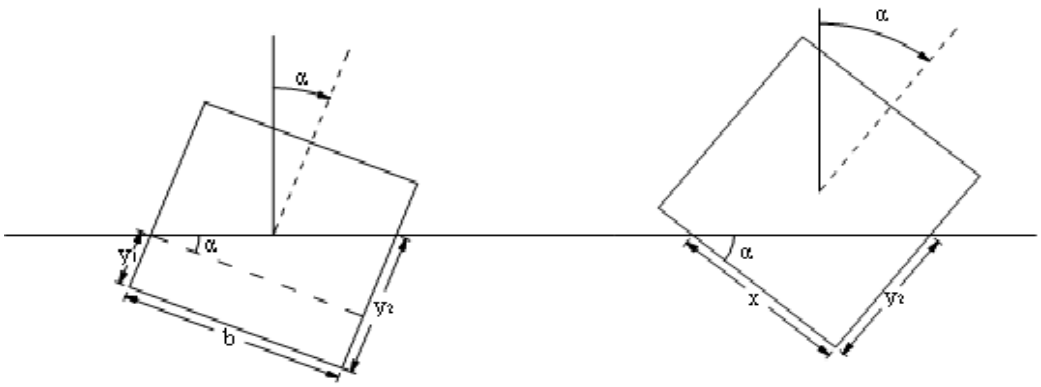

Figure 30: Values of the Fig. 31. [4]

$$Case\ a\text{: } tana = \frac{y_2 - y_1}{b}$$

$$Case\ b\text{: } tana = \frac{y_2}{x} = \frac{y_2}{y_1}$$

Square prism:

Height of the internal water (amount of h)	*y_1 (cm)*	*y_2 (cm)*	*a (deg)*
0.1h	8.2	16.7	24
0.15h	13.5	15.5	41
0.2h	13.9	13.9	45
0.4h	13.9	13.9	45
0.6h	13.9	13.9	45
0.8h	17.2	17.5	44
0.9h	20	20	0

Figure 31: Experimental measurements for the square prism.

Orthogonal prism

Height of the internal water (amount of h)	*y_1 (cm)*	*y_2 (cm)*	*a (deg)*
0.1h	4.3	6.3	5.8
0.15h	0.6	6.3	16
0.3h	14.6	15.6	47
0.55h	9.7	12.5	1.5
0.7h	18	18	0
0.9h	18	18	0

Figure 32: Experimental measurements for the orthogonal prism.

So, here we see:

a: angle of heel for the prism

y_1, y_2: dimensions as they are shown in Fig.38

u: height of the internal water

h: height of the prism

During the experiment, we observed that the prism was leaning either clockwise or counterclockwise. In order to distinguish the direction of the prisms, we consider the clockwise direction as the negative one (-a) and the counterclockwise direction as the positive one (a). This choice is in accordance with the previous, theoretical approach. Now, wanting to do the experimental process more understandable, we present some pictures:

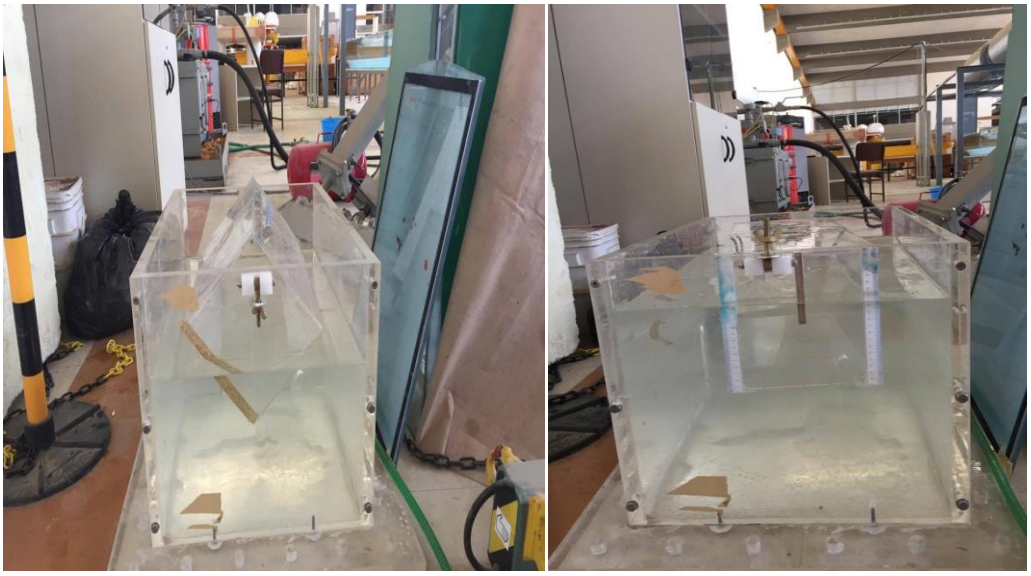

Figure 33: Pictures of the prism in a vertical and a leaning position of balance.

Figure 34: Longwise aspect of the prism in a leaning position of balance.

8.4 Comparison of the results

In this chapter, we are going to compare the mathematical and the experimental results. In order to do so, we created a graph in which our experimental results represented by dots and our analytical results represented by continuous curves are shown together. The experiments were conducted on a square prism (λ=1) and an orthogonal prism (λ=0.9), so we just had to create the graphs of these cases in MatLab.

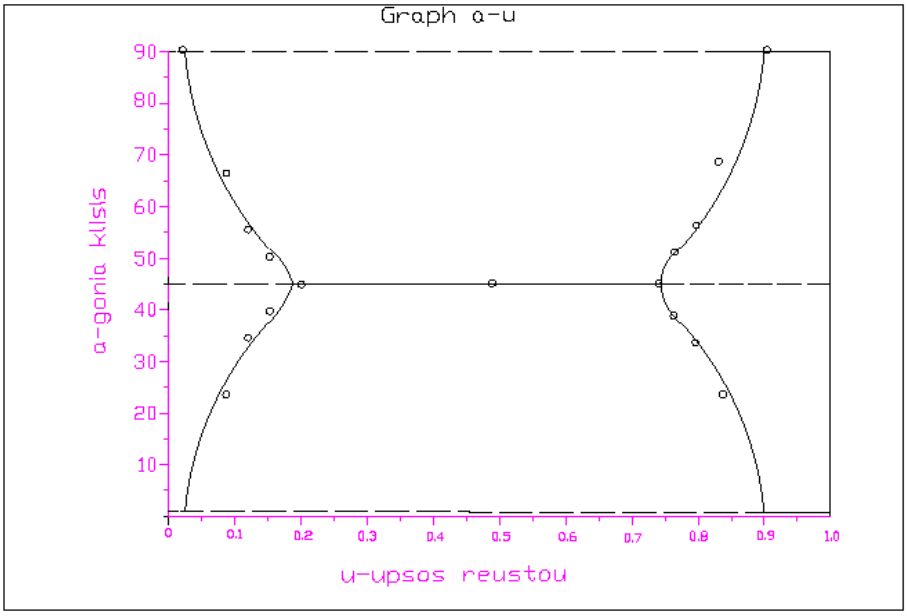

Figure 35: Experimental results and mathematical results for the square prim in one graphic.

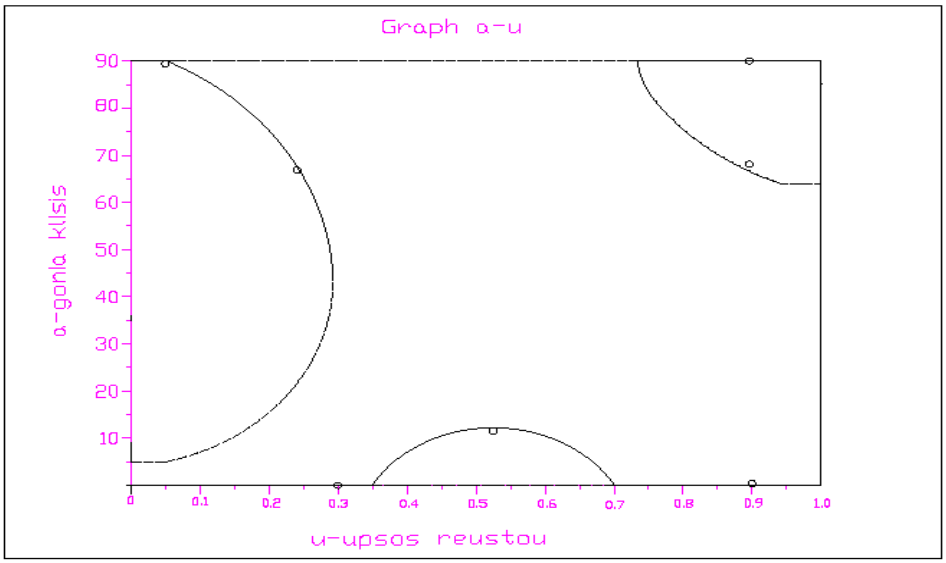

Figure 36: Experimental results and mathematical results for the orthogonal prim in one graphic.

Finally, we can safely conclude from the above figures that there is a convergence between the results. In particular, we observe:

- There are small differences between the mathematical and the experimental values, especially for high values of a.
- The point of the symmetry breaking is very close in the two approaches.
- The differences between the two approaches are caused by the experimental errors. More specifically:
    1. The geometrical characteristics of the models might differ from the theoretical values.
    2. The fact that the model used in the experiment had a finite length affected its behavior. This statement is true because during the experiment the orthogonal prism appeared to have trim for high values of u.
    3. Possible errors in measurement concerning both the weight and dimensions of the models.
    4. We also made the assumption that the mass density of the water is $\rho=1g/cm^3$, no matter the temperature of the room.
    5. The prism was dusty inside so the internal water was not pure.

9.0 Conclusions

In the present diploma thesis, we investigated the topic of static stability of orthogonal prisms (b × h × l) containing liquid in diverse, small or high, angles of heel. We started our study by reexamining the stability of prisms containing solid material. After that, we concentrated all the useful knowledge and conclusions from the previous study and we focused on the stability of prisms containing liquid. Our first approach was based on the energy method. The energy of the system prism-internal liquid-external liquid was studied in order to create some differential equations. By solving these equations, we plotted the diagrams a-u and a-r for different values of the other factors. The lack of theoretical sources on this issue or the lack of any previous similar studies created a sheer need of experimental confirmation. So, we conducted some experiments and studied the convergence between the results.

Summing up, the main conclusions of the present diploma thesis are:

- We studied the effect of factors such as the ratio of dimensions, the density ratio of external to internal liquid and the weight of the prisms to the stability. In this way, we perceived the importance of these factors. The change of value for each one of these parameters, no matter how small, can strongly affect the balance angle of the system.
- The initial metacentric height constitutes a limited power criterion. This is obvious from the fact that a positive initial metacentric height cannot ensure that the system balances on the vertical position.
- By alternating the parameters of the system, some interesting dynamic phenomena such as bifurcations occurred.
- We mainly deal with Pitchfork bifurcations and some saddle-node ones. In the case of the orthogonal prism, we are faced with imperfect bifurcations.
- By studying the results of the energy approach, we observe the famous symmetry breaking, that is, the phenomenon in which the symmetrical body balances on non-symmetrical positions.
- We found out a satisfying convergence between the theoretical and experimental results. Of course, there were some small differences mainly because of some experimental errors and assumptions.
- The most important error that we might have done was the assumption of infinite length of the prism. The orthogonal prism trimmed for high values of u (height of the internal liquid).

By comparing the results of the internal liquid case with the compact solid body case, we come to the following conclusions:

- The system presents similar behavior in both cases.

- The dynamic behavior of the systems is the same. In both cases bifurcations and symmetry breaking appeared.
- In the experimental approach of A. Sakellariou's study, the assumption of the infinite length was correct. In our case, it presented some errors.

Suggestions for further research:
The present diploma thesis could also expand in many other directions. Here, we mention some interesting suggestions:

- Study of stability for prisms of composite geometry (i.e. parabolic form of higher class).
- Study of stability for three-dimension bodies. In this way, the length is finite so one of the assumptions is rejected.
- Study of stability for a body of alternated geometry. This case study is much closer to a ship's geometry.
- Study of stability for bodies in a waved liquid environment.

References

1. Sakelariou A. (2013), Penetration in balance positions of floating bodies, Diploma thesis
2. Spyrou K. (2012), Ship Dynamic Stability, NTUA publication
3. Health T. L. (2002),The works of Archimedes, Dover Publications
4. Bouguer P. (1746) Traité du Navire, de sa Construction et de ses Mouvemens (Treatise of the Ship, its Construction and its Movements), Jombert, Paris
5. Euler L. (1967) Scientia Navalis seu Tractatus de Construendis ac Dirigendis Navibus (Science of Ships or Treatise on How to Build and Operate Ships), 2 vols., St. Petersburg, (1749). Republ in Euler's Collected Works, Series II, issued by the Euler Comm of the Swiss Academy of Natural Science, Zurich and Basel
6. https://www.sakketosaggelos.gr/Article/714/
7. Gilbert E. (1991), How things float, The American Monthly, Vol. 98, No 3, pp 201-216, Mathematical Association of America
8. Erdős P., Schibler G., Herndon R. C., (1992) Floating equilibrium of Symmetrical Objects and the breaking of symmetry. Part 1: Prisms, American Journal of Physics& Part 2: The cube, the octahedron , and the tetrahedron.
9. Netz R., Noel W. (2010) The story of the amazing discovery of Archimedes' lost works, Archimedes, The Palimpsest Project
10. http://www.marineinsight.com/naval-architecture
11. https://www.researchgate.net
12. http://www.delftship.net/
13. Tzabiras G (2007), Ship Hydrostatic and Stability I (Book 1), NTUA publication
14. Rawson K. J., Tupper E.C. (2001), Basic Ship Theory, Vol. 1, Longman Pub. Group
15. Paipeltis S. A., Ceccarelli Marco (2010), The Genius of Archimedes- 23 Centuries of Influence on Mathematics, Science and Engineering, Proceedings of an international conference held at Syracuse
16. Biran Adrian (2003), Ship Hydrostatics and Stability, Edition 1, Butterworth-Heinemann
17. Belenky V., Bassler C., Spyrou K. (2011), Development of second generation intact stability criteria, West Bethesda, Hydromechanics Department Report
18. Atwood G. (1796) The Construction and Analysis of Geometrical Propositions, Determining the Positions Assumed by Homogeneal Bodies which Float Freely, and at Rest, on a Fluid's Surface; Also Determining the Stab of Ships and of Other Float Bodies, Philos. Trans. of the R. Soc. of London
19. Atwood G, Vial du Clairbois HS (1798) A Disquisition on the Stability of Ships, Philos. Trans. of the R. Soc. of London, Vol. 88, vi-310
20. Dupin C.(1813),Développements de géometrie: avec des applications à la stabilité des vaisseaux, aux déblais et remblais, au défilement, à l'optique, etc. pour faire suite a la Géometrie descriptive et a la Géometrie analytique de M. Monge (Developments in geometry, with applications to the stability of vessels, to trenches and embankments, to ramparts, to optics, etc following

the Descriptive Geometry and Analytic Geometry of Mr. Mongue), Mme Ve Courcier, Paris

21. http://tutorial.math.lamar.edu/Classes/DE/PhasePlane.aspx
22. Strogatz S. H.(2000), *Nonlinear Dynamics and Chaos*, Perseus Book Publishing
23. https://www.math.ucdavis.edu
24. Dr. James H. Banks, Ph.D., The properties of fluids, Department of Civil and Environmental Engineering, San Diego State University
25. INTERNATIONAL MARITIME ORGANIZATION (IMO)- www.imo.org